2 μg of total RNA and Moloney murine leukemia virus reverse transcriptase (Promega). Using the cDNA as templates, PCR amplification was performed with primers as follows: ribozyme sense, 5′-TCC CCG GTT CGA AAC CGG GCA-3′; ribozyme antisense, 5′-GCT TGC ATG CCT GCA GGT CGA CGC GAT AGA AAA AAA GAT ATC CGG GGT-3′; β-actin sense, 5′-GCA CGG CAT CGT CAC CAA CT-3′; and β-actin antisense, 5′-AAG GCT GGA AGA GTG CCT CA-3′. The amplified fragments of DNA were confirmed by agarose gel electrophoresis. Fragments carrying ribozymes that were derived from the metastatic nodules were cloned into the pGEM-T vector (Promega) and sequenced.

Search of DNA Data Bases—By searching of mouse cDNA databases with the BLAST program, identification of target genes of the selected ribozymes was performed (22) (www3.ncbi.nlm.nih.gov/BLAST/). Parameters for the data base searches were set to optimize searches for short, nearly exact sequences.

Construction and Transfection of siRNA Expression Plasmid—Plasmid vectors encoding siRNAs for four of the eight identified targets were constructed as described (23). Two target sites for each of the genes were selected using an algorithm (www.igene-therapeutics.co.jp). Transfections were performed using LipofectAMINE Plus (Invitrogen). Typically, 3 μg of plasmid DNA was used per 80% confluent 6-cm dish culture. Transfected B16F0 cells were selected in medium containing puromycin (2.5 μg/ml) for 48 h and then subjected to RT-PCR analysis and *in vitro* scratch-wound assay. The expression of targeted genes was examined by gene-specific primers, *STIM1* (sense: 5′-GGG AAG ACC TCA ATT ACC A-3′ and antisense: 5′-CAG CTG CAG CTT CTG CCT GT-3′), *Polg-2* (sense: 5′-GGG AAG CAA ACT TTA CTA CAA CT-3′ and antisense: 5′-ATC CAA AGC GAC CTT AAT AG-3′), and *Cyp2d22* (sense: 5′-AAG GAG GAA GCT GGA TTC CTA CC-3′ and antisense: 5′-CCC TAT GAC TTC ATC GAT TT-3′), on standard condition for RT-PCR (25 cycles of 94 °C for 30 s, −54 °C for 60 s, −72 °C for 60 s).

Scratch-wound Assay—B16F0 cells that had been treated with siRNA expression plasmid were allowed to form a monolayer on a fibronectin (10 μg/ml)-coated dish surface. A wound was made in the monolayer of cells by completely scratching the cells in a line with a pipette tip. Cells were washed a few times with PBS to remove cell debris and fed with fresh medium as described (14). The time of the scratching wound was designated as time 0. Cells were allowed to proliferate and migrate into the wound during the next 30 h. Migration of cells into the wound was recorded under a phase contrast microscope with a 10× phase objective.

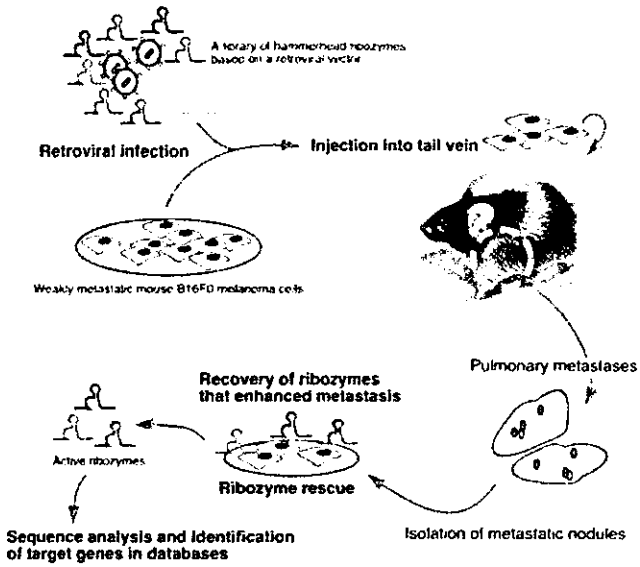

FIG. 1. **Strategy for the identification of genes using a randomized library of hammerhead ribozymes and the assay *in vivo* for the determination of the metastatic potential of melanoma cells.**

RESULTS AND DISCUSSION

We constructed a library of ribozymes that was based on the retroviral expression vector pMXpuro (20). Retroviruses carrying randomized ribozymes were prepared in the packaging cell line Plat-E as described elsewhere (14, 20). Then we infected weakly metastatic B16F0 cells with the retroviruses for the selection of ribozymes that enhanced the metastatic properties

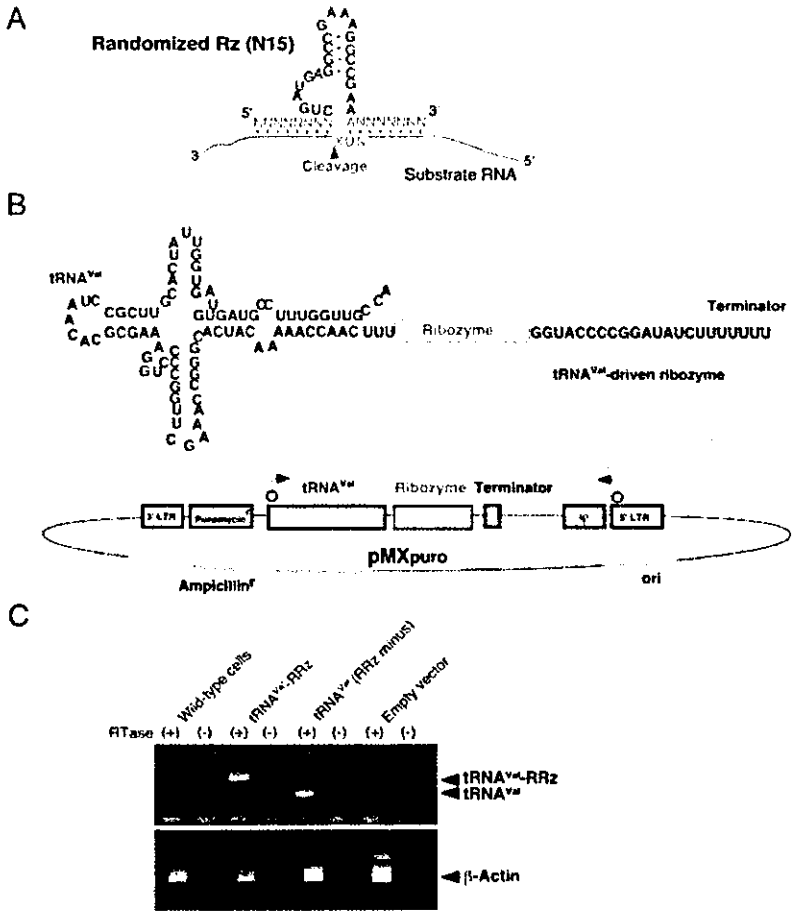

FIG. 2. **The randomized ribozyme.** *A*, *red letters* indicate the randomized recognition arms of the hammerhead ribozyme (*Rz*). Substrate RNAs contain a NUX triplet (where N and *X* represent A, U, G, or C and A, U, or C, respectively) that is susceptible to cleavage by hammerhead ribozymes (3). *B*, the structure of the retroviral vector, pMXpuro, that carried the randomized ribozymes. Ribozymes were expressed as $tRNA^{Val}$-fused RNAs. *LTR*, long terminal repeat. *C*, cells were infected with retroviruses that carried a $tRNA^{Val}$-fused randomized ribozyme (*RRz*) or $tRNA^{Val}$ alone (*RRz minus*) or with the empty vector (*$tRNA^{Val}$* and *RRz minus*). The expression of $tRNA^{Val}$-fused RRz or $tRNA^{Val}$ (*RRz minus*) was confirmed by RT-PCR analysis. Results of RT-PCR for β-actin mRNA are also shown as internal controls. Symbols (+) and (−) refer to assays with and without reverse transcriptase (*RTase*). Cells infected with the retrovirus that carried $tRNA^{Val}$ alone (*RRz minus*) were used as controls in subsequent experiments.

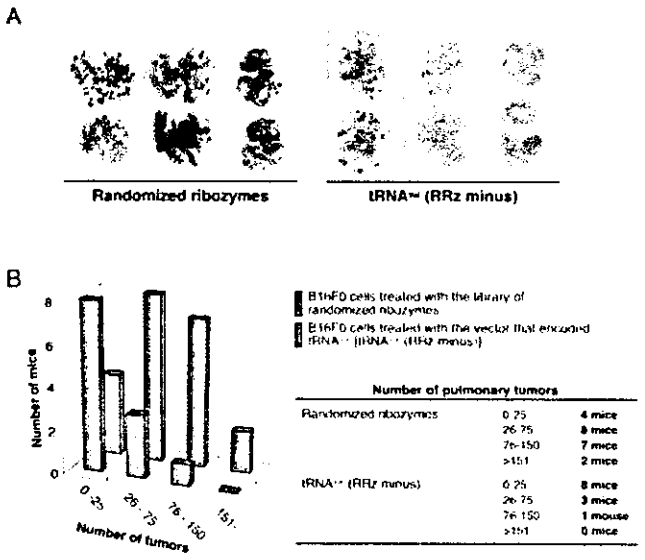

FIG. 3. **Selection *in vivo* of ribozymes that enhanced the metastatic properties of B16F0 melanoma cells, using a mouse model and cells treated with the library of randomized ribozymes.** *A*, isolation of pulmonary metastases. *B*, number of pulmonary tumors isolated after the injection of B16F0 cells that had been treated with randomized ribozymes (*RRz*) or tRNA^{Val} alone (*RRz minus*).

TABLE I
Selected ribozymes and their target genes

Selected ribozymes and their target genes

	Recognition arm		Recognition arm
RRzA:	ATCGATCG		AGTCTCCC
RRzB:	CTGCGTTG		ATTGGATT
RRzC:	CTTTCGCG		ATACGAAC
RRzD:	GCGCGGAG		ACAGGTAT
RRzE:	GCTTCCCC		ACGTGAGG
RRzF:	GGATGGGC		ATCCCCAT
RRzG:	GTACCCGC		ACGTGTGG
RRzH:	GTCGACCA		ATTGTAGC

Target sequence	Target gene
RRzA GGGAGACTNCGATCGAT	*Mus musculus* stromal interaction molecule 1, (cDNA clone MGC:13964 IMAGE:4191156) GenBank accession number: BC021644.1
RRzB AATCCAATNCAACGCAG	*Mus musculus* expressed sequence AW551984 (AW551984) GenBank accession number: NM_178737.1
RRzC GTTCGTATNCGCGAAAG	*Mus musculus* polymerase (DNA-directed), gamma 2, accessory subunit (Polg2) GenBank accession number: NM_015810.1
RRzD ATACCTGTNCTCCGCGC	*Mus musculus* cytochrome P450, family 2, subfamily d, polypeptide 22 (Cyp2d22) GenBank accession number: NM_019823.1
RRzE CCTCACGTNGGGGAAGC	*Mus musculus* LOC230840 (LOC230840) GenBank accession number: XM_161442.1
RRzF ATGGGGATNGCCCATCC	*Mus musculus* hypothetical gene; supported by AK030301 (LOC328981) GenBank accession number: XM_286862.1
RRzG CCACACGTNGCGGGTAC	Unidentified
RRzH CCTACAATNTGGTCGAC	*Mus musculus* hypothetical gene; supported by AK040634 (LOC329840) GenBank accession number: XM_287326.1

of the cells (Fig. 2, *A* and *B*). After antibiotic (puromycin) selection, we confirmed the expression of randomized ribozymes in cells by RT-PCR analysis with primers specific for the parent ribozyme (Fig. 2*C*). Then we injected 5×10^5 control or randomized ribozymes harboring B16F0 cells intravenously into the lateral tail vein of individual C57BL/6N mice. Cells with enhanced metastatic properties were selected by their isolation from lung as pulmonary tumors. Only a few pulmonary metastases were detected in the mice injected with parent B16F0 cells as reported earlier (18, 19). Fig. 3, *A* and *B*, show the difference in terms of the resultant pulmonary metastases

TABLE II
siRNA target sequence

Gene	Target site	Sequence
STIM1	Site 1	GGGAAGACCTCAATTACCA
	Site 2	GGCCAAGAAGACATTTATA
AW551984	Site 1	GAACAAACTTCTATCTTTA
	Site 2	AGTCAAACTTGTAAATAGA
Polg2	Site 1	GAAGCAAACTTTACTACAA
	Site 2	GGGAAAGGAGCCAATAGAA
Cyp2d22	Site 1	GAAGGAAACTCTTAAGGAA
	Site 2	GCGCCGAGTACAACAGGAA

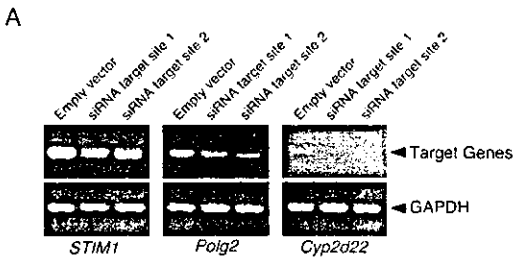

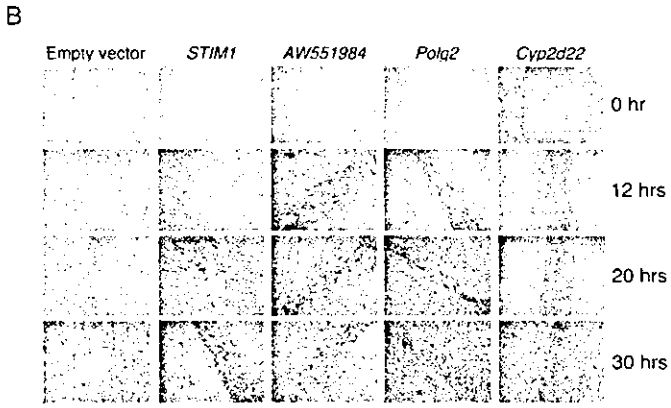

FIG. 4. **Silencing of *STIM1*, *AW551984*, *Polg2*, and *Cyp2d22* by siRNA expression vector.** *A*, expression levels of target genes were confirmed by RT-PCR analysis. Results of RT-PCR for glyceraldehyde-3-phosphate dehydrogenase (*GAPDH*) mRNA are also shown as internal controls. *B*, scratch-wound assay. Movement of cells into the wound is shown for cells transfected with empty vector (control) or siRNA expression vectors (target site 2) against *STIM1*, *AW551984*, *Polg2*, and *Cyp2d22*.

between cells that had been treated with the ribozyme library and untreated cells, 2 weeks after injection. The number of metastatic melanoma nodules derived from library-treated cells was clearly higher than those derived from untreated cells. Thus, certain ribozymes in the library appeared to have promoted the pulmonary metastasis of B16F0 cells (Fig. 3, *A* and *B*).

Next, we removed the pulmonary nodules of melanoma cells derived from ribozyme harboring cells (Fig. 3*A*), and we collected cells from these nodules by mincing and treating them with trypsin. The resultant cells were cultured, and RNA was isolated from these cells. Then ribozymes were amplified by RT-PCR strategy and cloned into plasmid vector (15) (Fig. 1), and the results of sequencing of the ribozymes indicated that the selected ribozymes represented eight types of ribozyme that contained specific substrate-recognition arms (Table I). By this way, we recovered ribozymes that appeared to have raised the metastatic potential of B16F0 cells.

We then identified their target genes by searching data bases with the BLAST program, using settings that optimized searches for short, nearly exactly matching sequences (22) (www3.ncbi.nlm.nih.gov/BLAST/) (Table I). Among the selected ribozymes, our search indicated that ribozyme A targeted the transcript of the gene known as stromal interaction molecule 1 (*STIM1*). *STIM1* is a gene for a transmembrane glycoprotein. This gene is located at human chromosome region 11p15.5, which is involved in tumorigenesis. Moreover, overexpression of *STIM1* causes growth arrest and cell death in several lines of cells (24, 25). These earlier observations indicate that *STIM1* functions as a tumor suppressor. Therefore, our identification of a ribozyme that targets *STIM1* in our assay of metastasis by cells treated with a ribozyme library seems eminently reasonable. Our data base search also identified genes whose functions have not yet been well characterized, such as the sequence AW551984, expressed in the mouse, which contains a VWA domain that seems to mediate adhesion of eukaryotic cells (a target for ribozyme B; GenBank™ accession number NM_178737.1; Table I).

We next constructed siRNA expression vectors against four (*STIM1*, *AW551984*, *Polg2*, and *Cyp2d22*) out of the eight identified genes and examined their functional involvement in metastasis by carrying out a scratch-wound assay that is commonly used to study the ability of cells to migrate (26, 27), a reliable parameter for metastasis. We prepared two different siRNA expression vectors for each of target genes (Table II). Cells harboring the expression plasmid were selected in puromycin supplemented medium. We examined suppression of the expression of target genes and confirmed reduced levels of expression of three genes, *STIM1*, *Polg2*, and *Cyp2d22* (unfortunately, *AW551984* transcript could not be detected by RT-PCR analysis) (Fig. 4*A*). Then we subjected the cells to the scratch-wound assay (Fig. 4*B*). Targeting of all the four genes led to significant acceleration of migration, which is one of the properties of metastatic cells. *AW551984*- and *Polg2*-targeted B16F0 cells moved more than 90% of the width of the wound in 30 h, whereas control cells, which had been treated with empty vector, only initiated to migrate into the wound. Parallel observation on *STIM1*- and *Cyp2d22*-targeted cells revealed about 50% movement into the wound (Fig. 4*B*). Although siRNA-induced suppression of *AW551984* could not be confirmed due to technical difficulty in RT-PCR analysis, the change in phenotype (increased migration) was obtained in two independent experiments. Taken together, these four genes appeared to have a role in control of the metastatic properties of B16F0 melanoma cells. Further investigation of genes identified in this study would provide important clues to the complex mechanism(s) of metastasis.

To the best of our knowledge, this is the first demonstration of the applicability of a ribozyme library to the identification of genes using animal model. To date, such a potential has been demonstrated only in cultured cells (7–15, 28, 29). It should now be possible to identify important functional genes *in vivo* using randomized ribozyme libraries.

Acknowledgments—We thank Dr. Toshio Kitamura (Institute of Medical Science, University of Tokyo) for supplying the retroviral vector pMXpuro and the packaging cell line Plat-E, as well as Drs. Motowo Nakajima and Tatsuhiko Kasaoka (Tsukuba Research Institute, Novartis Pharma, Tsukuba Science City) for critical comments and helpful discussions.

REFERENCES

1. Uhlenbeck, O. C. (1987) *Nature* **328,** 596–600
2. Haseloff, J., and Gerlach, W. L. (1988) *Nature* **334,** 585–591
3. Zhou, D. M., and Taira, K. (1998) *Chem. Rev.* **98,** 991–1026
4. Kawasaki, H., Eckner, R., Yao, T. P., Taira, K., Chiu, R., Livingston, D. M., and Yokoyama, K. K. (1998) *Nature* **393,** 284–289
5. Gasteland, R. F., Cech, T. R., and Atkins, J. F. (1999) *The RNA World*, 2nd Ed., Cold Spring Harbor Laboratory Press, Cold Spring Harbor, NY
6. Krupp, G., and Gaur, R. K. (2000) *RIBOZYME: Biochemistry and Biotechnology*, Eaton Publishing, Natick, MA
7. Kruger, M., Beger, C., Li, Q. X., Welch, P. J., Tritz, R., Leavitt, M., Barber, J. R., and Wong-Staal, F. (2000) *Proc. Natl. Acad. Sci. U. S. A.* **97,** 8566–8571
8. Li, Q. X., Robbins, J. M., Welch, P. J., Wong-Staal, F., and Barber, J. R. (2000) *Nucleic Acids Res.* **28,** 2605–2612
9. Welch, P. J., Marcusson, E. G., Li, Q. X., Beger, C., Kruger, M., Zhou, C., Leavitt, M., Wong-Staal, F., and Barber, J. R. (2000) *Genomics* **66,** 274–283
10. Beger, C., Pierce, L. N., Kruger, M., Marcusson, E. G., Robbins, J. M., Welcsh, P., Welch, P. J., Welte, K., King, M. C., Barber, J. R., and Wong-Staal, F. (2001) *Proc. Natl. Acad. Sci. U. S. A.* **98,** 130–135
11. Kawasaki, H., Onuki, R., Suyama, E., and Taira, K. (2002) *Nat. Biotechnol.* **4,** 376–380
12. Kawasaki, H., and Taira, K. (2002) *EMBO Rep.* **3,** 443–450
13. Suyama, E., Kawasaki, H., Kasaoka, T., and Taira, K. (2003a) *Cancer Res.* **63,** 119–124
14. Suyama, E., Kawasaki, H., Nakajima, M., and Taira, K. (2003b) *Proc. Natl. Acad. Sci. U. S. A.* **100,** 5616–5621
15. Nelson, L. D., Suyama, E., Kawasaki, H., and Taira, K. (2003) *Targets* **2,** 191–200
16. Tannock, I. F., and Hill, R. P. (1998) *The Basic Science of Oncology*, 3rd Ed., The McGraw-Hill Companies, New York
17. Holland, J. F., and Frei, E. (2000) *Cancer Medicine*, 5th Ed., B. C. Decker, Hamilton, Canada
18. Fidler, I. J. (1973) *Nat. New Biol.* **242,** 148–149
19. Clark, E. A., Golub, T. R., Lander, E. S., and Hynes, R. O. (2000) *Nature* **406,** 532–535
20. Morita, S., Kojima, T., and Kitamura, T. (2000) *Gene Ther.* **7,** 1063–1066
21. Koseki, S., Tanabe, T., Tani, K., Asano, S., Shioda, T., Nagai, Y., Shimada, T., Ohkawa, J., and Taira, K. (1999) *J. Virol.* **73,** 1868–1877
22. Altschul, S. F., Madden, T. L., Schaffer, A. A., Zhang, J., Zhang, Z., Miller, W., and Lipman, D. J. (1997) *Nucleic Acids Res.* **25,** 3389–3402
23. Wadhwa, R., Kaul, S. C., Miyagishi, M., and Taira, K. (2004) *Rev. Mutat. Res.*, in press
24. Sabbioni, S., Barbanti-Brodano, G., Croce, C. M., and Negrini, M. (1997) *Cancer Res.* **57,** 4493–4497
25. Manji, S. S., Parker, N. J., Williams, R. T., van Stekelenburg, L., Pearson, R. B., Dziadek, M., and Smith, P. J. (2000) *Biochim. Biophys. Acta* **1481,** 147–155
26. Magdalena, J., Millard, T. H., and Machesky, L. M. (2003) *J. Cell Sci.* **116,** 743–756
27. Ettenson, D. S., and Gotileb, A. I. (1995) *Arterioscler. Thromb. Vasc. Biol.* **15,** 515–521
28. Onuki, R., Bando, Y., Suyama, E., Katayama, T., Kawasaki, H., Baba, T., Tohyama, M., and Taira, K. (2004) *EMBO J.* **23,** 959–968
29. Kuwabara, T., Hsieh, J., Nakashima, K., Taira, K., and Gage, F. H. (2004) *Cell* **116,** 779–793

J|A|C|S
ARTICLES
Published on Web 11/09/2004

NMR-Based Reappraisal of the Coordination of a Metal Ion at the Pro-*Rp* Oxygen of the A9/G10.1 Site in a Hammerhead Ribozyme

Ken-ichi Suzumura,[†] Yasuomi Takagi,[‡] Masaya Orita,[†] and Kazunari Taira*[,§,∥]

Contribution from the Yamanouchi Pharmaceutical Co., Ltd., 21 Miyukigaoka, Tsukuba Science City, 305-8585, Japan, iGENE Therapeutics Inc., Central 4, 1-1-1 Higashi, Tsukuba Science City, 305-8562, Japan, Gene Function Research Center, National Institute of Advanced Industrial Science and Technology (AIST), Tsukuba Central 4, 1-1-1 Higashi, Tsukuba Science City, 305-8562, Japan, and Department of Chemistry and Biotechnology, School of Engineering, The University of Tokyo, 7-3-1 Hongo, Tokyo 113-8656, Japan

Received May 9, 2004; E-mail: taira@chembio.t.u-tokyo.ac.jp

Abstract: In the identification of a metal-binding site within enzymes, kinetic analyses based on thio-effects and Cd^{2+}-rescues are widely used. In those analyses, kinetic studies using a phosphorothioate have been discussed on the premise that the substitution by a sulfur atom does not change the conformation of a ribozyme. However, our present NMR structural analysis demonstrates the change of the conformation at the metal-binding site by ***Rp***-sulfur but not by ***Sp***-sulfur substitution and warns against incautious interpretations of thio-effects and rescue phenomena in kinetic studies using a phosphorothioate. Our analysis further demonstrates that, in solution, a Cd^{2+} ion can interact with an ***Rp***-phosphorothioate (in support of the controversial McKay's structure, *Nature* **1994**, *372*, 68−74) and with an ***Sp***-phosphorothioate (in support of the controversial Scott's structure, *Cell* **1995**, *81*, 991−1002) at the metal-binding A9/G10.1 site and that, in the former case, the bound Cd^{2+} ion can return the ribozyme to an active conformation and rescue its enzymatic activity.

The hammerhead ribozyme is a self-cleaving RNA that is found in small RNA plant pathogens, and it catalyzes the sequence-specific cleavage of RNA. Metal ions play an important role in the catalytic cleavage of the phosphodiester bond in an RNA by hammerhead ribozymes and the reaction yields a 2′,3′-cyclic phosphate.[1] Studies by X-ray crystallography have facilitated analysis of the mechanism of action of these ribozymes.[2] The crystal structure obtained by McKay's group revealed a metal-binding site, A9/G10.1, located in the vicinity of domain II, which forms a continuous stack between stem II and stem III.[2a] In this crystal structure, an Mn^{2+} ion binds between the pro-***Rp*** oxygen of the phosphate group of A9 (P9 oxygen) and the N7 atom of G10.1. Even though this metal-binding site (A9/G10.1 site) within the crystal structure is located approximately 20 Å from the scissile phosphodiester bond, this metal-binding site is thought to play a crucial role in achieving maximal cleavage activity for the following reasons. Replacement of the pro-***Rp***-phosphoryl P9 oxygen atom by a sulfur atom results in a dramatic decrease in Mg^{2+}-dependent catalytic activity.[3] Furthermore, replacement of G10.1 by a pyrimidine also results in a substantial decrease in the ribozyme's activity.[4] Moreover, the addition of a low concentration of Cd^{2+} ions, which are thiophilic, to a solution of the ribozyme with an ***Rp***-phosphorothioate linkage returns the rate of the catalytic reaction to the control value.[5]

[†] Yamanouchi Pharmaceutical Co., Ltd.

[‡] iGENE Therapeutics Inc.

[§] Gene Function Research Center, National Institute of Advanced Industrial Science and Technology.

[∥] Department of Chemistry and Biotechnology, School of Engineering, The University of Tokyo.

(1) (a) Lilley, D. M. J. *Curr. Opin. Struct. Biol.* **1999**, *9*, 330−338. (b) Scott, E. C.; Uhlenbeck, O. C. *Nucleic Acids Res.* **1999**, *27*, 479−484. (c) Wang, S.; Karbstein, K.; Peracchi, A.; Beigelman, L.; Herschlag, D. *Biochemistry* **1999**, *38*, 14363−14378. (d) Murray, J. B.; Scott, W. G. *J. Mol. Biol.* **2000**, *296*, 33−41. (e) Nakamatsu, Y.; Kuwabara, T.; Warashina, M.; Tanaka, Y.; Yoshinari, K.; Taira, K. *Genes Cells* **2000**, *5*, 603−612. (f) O'Rear, J. L.; Wang, S.; Feig, A. L.; Beigelman, L.; Uhlenbeck, O. C.; Herschlag, D. *RNA* **2001**, *7*, 537−545. (g) Curtis, E. A.; Bartel, D. P. *RNA* **2001**, *7*, 546−552. (h) Takagi, Y.; Warashina, M.; Stec, W. J.; Yoshinari, K.; Taira, K. *Nucleic Acids Res.* **2001**, *29*, 1815−1834. (i) Hammann, C.; Norman, D. G.; Lilley, D. M. J. *Proc. Natl. Acad. Sci. U.S.A.* **2001**, *98*, 5503−5508 (j) Burke, J. M. *Biochem. Soc. Trans.* **2002**, *30*, 1115−1118. (k) Hammann, C.; Lilley, D. M. J. *ChemBioChem* **2002**, *3*, 690−700. (l) Zhou, J. M.; Zhou, D. M.; Takagi, Y.; Kasai, Y.; Inoue, A.; Baba, T.; Taira, K. *Nucleic Acids Res.* **2002**, *30*, 2374−2382. (m) Inoue, A.; Takagi, Y.; Taira, K. *Magnes. Res.* **2003**, *16*, 210−217. (n) Takagi, Y.; Ikeda, Y.; Taira, K. *Topics Curr. Chem.* **2004**, *232*, 213−251. (o) Warashina, M.; Kuwabara, T.; Nakamatsu, Y.; Takagi, Y.; Kato, Y.; Taira, K. *J. Am. Chem. Soc.* **2004**, *126*, 12291−12297. (p) Takagi, Y.; Inoue, A.; Taira, K. *J. Am. Chem. Soc.* **2004**, *126*, 12856−12864.

(2) (a) Pley, H. W.; Flaherty, K. M.; McKay, D. B. *Nature* **1994**, *372*, 68−74. (b) Scott, W. G.; Finch, J. T.; Klug, A. *Cell* **1995**, *81*, 991−1002. (c) Scott, W. G.; Murray, J. B.; Arnold, J. R. P.; Stoddard, B. L.; Klug, A. *Science* **1996**, *274*, 2065−2069. (d) Murray, J. B.; Terwey, D. P.; Maloney, L.; Karpeisky, A.; Usman, N.; Beigelman, L.; Scott, W. G. *Cell* **1998**, *92*, 665−673. (e) Murray, J. B.; Szöke, H.; Szöke, A.; Scott, W. G. *Mol. Cell* **2000**, *5*, 279−287. (f) Scott, W. G. *J. Mol. Biol.* **2001**, *311*, 989−999. (g) Murray, J. B.; Dunham, C. M.; Scott, W. G. *J. Mol. Biol.* **2002**, *315*, 121−130.

(3) Ruffner, D. E.; Uhlenbeck, O. C.; *Nucleic Acids Res.* **1990**, *18*, 6025−6029.

(4) (a) Ruffner, D. E.; Stormo, G. D.; Uhlenbeck, O. C. *Biochemistry* **1990**, *29*, 10695−10702. (b) Tuschl, T.; Eckstein, F. *Proc. Natl. Acad. Sci. U.S.A.* **1993**, *90*, 6991−6994.

(5) Peracchi, A.; Beigelman, L.; Scott, E. C.; Uhlenbeck, O. C.; Herschlag, D. *J. Biol. Chem.* **1997**, *272*, 26822−26826.

10.1021/ja0472937 CCC: $27.50

The results of crystallographic and kinetic studies have indicated that binding of a metal ion at the pro-***Rp*** oxygen of A9/G10.1 site is of critical importance for enzymatic catalysis by hammerhead ribozymes.[2a,5] However, this conclusion remains controversial. For example, in the crystal structure obtained by Scott's group, the metal ion does not bind at the pro-***Rp*** oxygen but, instead, it binds at the pro-***Sp*** oxygen. To be specific, $Mg(H_2O)_5^{2+}$ binds directly to the pro-***Sp*** oxygen of A9 and is associated, via the hydration shell, with the exocyclic oxygen O6 of G8, with N7 of G10.1, and with N2 of G12.[2b] This potential $Mg(H_2O)_5^{2+}$-binding site corresponds to the Mn^{2+}-binding site identified by McKay's group in their crystal structure of a hammerhead ribozyme. Furthermore, ^{31}P NMR studies using phosphorothioates indicated that a metal ion binds to both the pro-***Sp*** and pro-***Rp*** oxygen. The ^{31}P NMR signals from ***Rp***- and ***Sp***-phosphorothioates at A9 in hammerhead ribozymes moved 2−3 ppm upfield shift upon the addition of one to two molar equivalents of Cd^{2+} ions.[6] Finally, in studies of the metal-binding motifs GA10***Sp***S and GA10***Rp***S, we found that binding of a metal ion was supported at both the pro-***Sp*** and the pro-***Rp*** position.[7]

The oligomers designated GA10***Sp***S and GA10***Rp***S are derivatives of the well-characterized GA10 oligomer,[8] whose sequence is shown in Figure 1, and they have a phosphorothioate group at A6, which corresponds to the A9 metal-binding site of a hammerhead ribozyme. Even though GA10 corresponds to the structure of only part of a hammerhead ribozyme-substrate complex (R32−S11; Figure 1), GA10 is analogous to the A9/G10.1 motif of the hammerhead ribozyme since GA10 includes a sheared-type tandem G12-A9 pair as a metal-binding site in the duplex, and it has been demonstrated that the GA10 molecule is sufficient to allow capture of divalent cations in the absence of any of the other conserved residues that are found in hammerhead ribozymes.[8b,c,d]

In our previous study, to clarify the functions of the pro-***Rp*** and the pro-***Sp*** positions at the cleavage site and the A9/G10.1 metal-binding site of the hammerhead ribozyme, we employed GA10***Sp***S and GA10***Rp***S as metal-binding motifs at the A9/G10.1 site.[7] The ^{31}P signals from both the ***Rp***- and the ***Sp***-phosphorothioate of GA10***Sp***S and of GA10***Rp***S moved considerably upfield upon the addition of Cd^{2+} ions to solutions of GA10***Rp***S and GA10***Sp***S. At 9 molar equiv of Cd^{2+} ions, the extent of perturbations of the phosphorothioate signals were close to the maximum, indicating saturation by Cd^{2+} ions of both GA10***Rp***S and GA10***Sp***S. At saturation (9 molar equiv Cd^{2+} ions), the chemical shifts were 10 and 6 ppm higher than those of GA10***Rp***S and GA10***Sp***S, respectively, in the absence of Cd^{2+} ions. Our previous studies with GA10***Sp***S and GA10***Rp***S also demonstrated that a Cd^{2+} ion is able to bind to both the ***Sp*** and the ***Rp*** sulfur atom in the absence of domain I (catalytic domain, formation by C3, U4, G5, A6, and C17 in Figure 1) of the hammerhead ribozyme. However, the nature and the conformation of the metal-binding sites in the presence of ***Rp***- and ***Sp***-phosphorothioates and in the absence of bound metal ions remain to be investigated. The exact effects of metal ions at the catalytically significant P9 site and their roles in the catalytic activity of hammerhead ribozymes remain to be clarified.

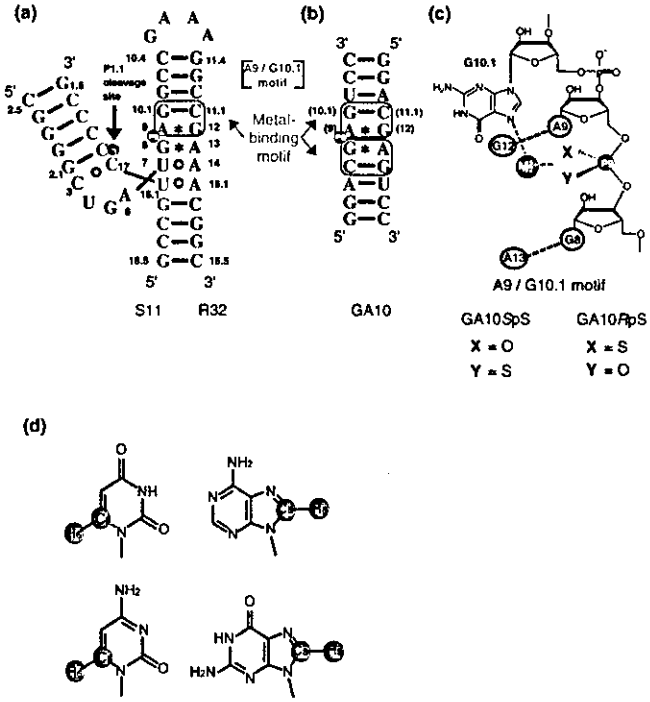

Figure 1. Sequences and secondary structures of (a) a hammerhead ribozyme (R32) and its substrate (S11). The black arrow indicates the cleavage site. (b) Sequence and secondary structure of GA10. The metal-binding motifs (the A9/G10.1 motif of the hammerhead ribozyme) are surrounded by magenta lines. In panels (a) and (b), Watson−Crick base pairs, non-Watson−Crick base pairs, and sheared-type G:A pairs are indicated by bars, open circles, and asterisks, respectively. GA10***Sp***S and GA10***Rp***S each have a phosphorothioate moiety at the A6 position, which corresponds to the A9 position of the hammerhead ribozyme. (c) Schematic representation of the A9/G10.1 motif. (d) Atoms in nucleobases that were monitored in natural-abundance $^1H-^{13}C$ HSQC.

Previous NMR investigations on the effects of a phosphorothioate on RNA structure led to two different conclusions.[9] One group observed a conformational change within an RNA hairpin by the introduction of an ***Rp***-phosphorothioate at the binding site of the phage MS2 capsid protein.[9a] The other group did not observe any structural changes by an ***Sp***-phosphorothioate modification at the metal binding site of yeast U6 RNA.[9b] The corresponding detailed structural study has not been performed for the hammerhead ribozyme with a phosphorothioate at the metal binding site, although limited ^{31}P NMR studies were reported.[6,7] In the present analysis, to elucidate the mechanism of binding of metal ions in the vicinity of the phosphate group at A9/G10.1, we examined the physicochemical properties of GA10***Sp***S and GA10***Rp***S by ^1H NMR, ^{31}P NMR, and $^1H-^{13}C$ HSQC spectroscopy. The ^1H, ^{13}C, and ^{31}P NMR signals of GA10***Sp***S in the absence and in the presence of Cd^{2+} ions were, respectively, similar to those of the unmodified parental RNA,

(6) Maderia, M.; Hunsicker, L. M.; DeRose, V. J. *Biochemistry* **2000**, *40*, 12113−12120.
(7) Suzumura, K.; Yoshinari, K.; Tanaka, Y.; Takagi, Y.; Kasai, Y.; Warashina, M.; Kuwabara, T.; Orita, M.; Taira, K. *J. Am. Chem. Soc.* **2002**, *124*, 8230−8236.
(8) (a) Katahira, M.; Kanagawa, M.; Sato, H.; Uesugi, S.; Fujii, S.; Kohno, T.; Maeda, T. *Nucleic Acids Res.* **1994**, *22*, 2752−2759. (b) Tanaka, Y.; Morita, E. H.; Hayashi, H.; Kasai, Y.; Tanaka, T.; Taira, K. *J. Am. Chem. Soc.* **2000**, *122*, 11303−11310. (c) Tanaka, Y.; Kojima, C.; Morita, E. H.; Kasai, Y.; Yamasaki, K.; Ono, A.; Kainosho, M.; Taira, K. *J. Am. Chem. Soc.* **2002**, *124*, 4595−4601. (d) Tanaka, Y.; Kasai, Y.; Mochizuki, S.; Wakisaka, A.; Morita, E. H.; Kojima, C.; Toyozawa, A.; Kondo, Y.; Taki, M.; Takagi, Y.; Inoue, A.; Yamasaki, K.; Taira, K. *J. Am. Chem. Soc.* **2004**, *126*, 744−752.
(9) (a) Smith, J. S.; Nikonowicz, E. P. *Biochemistry* **2000**, 39, 5642−5652. (b) Reiter, N. J.; Nikstad, L. J.; Allmann, A. M.; Johnson, R. J.; Butcher, S. E. *RNA* **2003**, 9, 533−542.

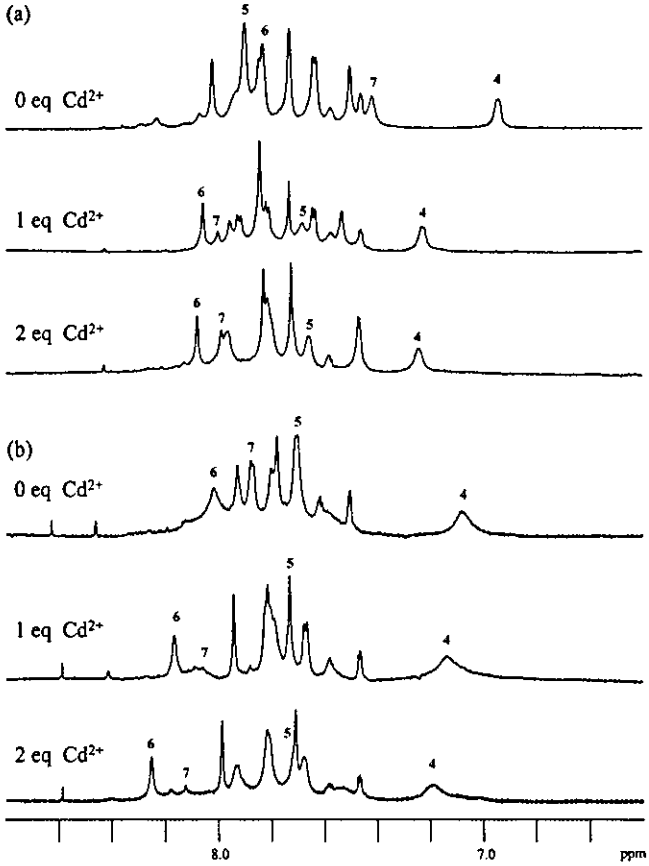

Figure 2. ^{1}H NMR spectra of GA10*Sp*S (a) and GA10*Rp*S (b). The spectra were recorded from samples dissolved in a solution of 40 mM $NaClO_4$ in 10 mM sodium cacodylate buffer at pH 7.6 in a 3-mm NMR tube at 40 °C. The concentrations, as duplexes, of GA10*Sp*S and GA10*Rp*S were 1.77 mM and 1.62 mM, respectively. From the top to the bottom in (a) and (b), the number of molar equivalents of $CdCl_2$ relative to the RNA was 0, 1, and 2, as indicated. Important signals of H8/H6 protons are labeled with respective residue numbers.

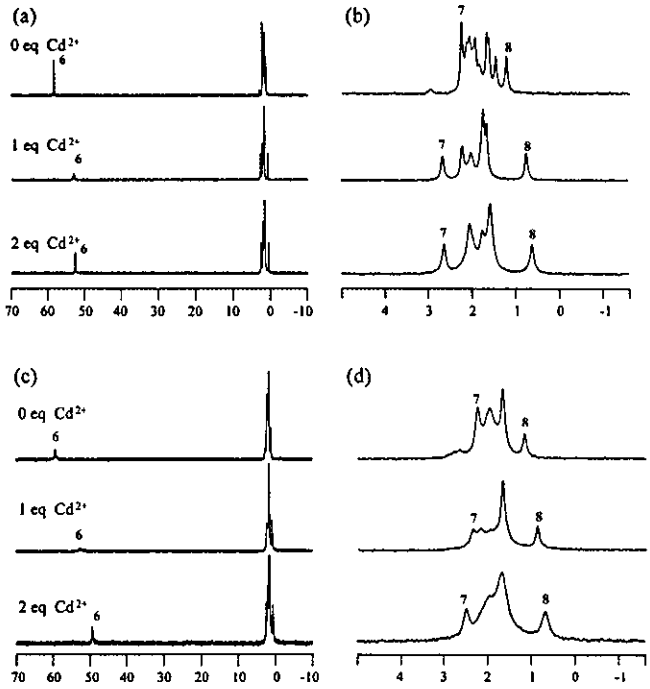

Figure 3. ^{31}P NMR spectra of GA10*Sp*S (a) and GA10*Rp*S (c). Expanded regions of the spectra are displayed in (b) and (d), respectively. The spectra were recorded from solutions of 40 mM $NaClO_4$ in 10 mM sodium cacodylate buffer at pH 7.6 in a 3-mm NMR tube at 40 °C. The concentrations, as a duplex, of GA10*Sp*S and GA10*Rp*S were 1.77 mM and 1.62 mM, respectively. From the top to the bottom in each group, the number of molar equivalents of $CdCl_2$ relative to the RNA was 0, 1, and 2, as indicated. With increasing concentrations of Cd^{2+} ions, signals from both the *Rp*- and the *Sp*-phosphorothioate (*Sp*, 58.5 ppm; and *Rp*, 59.7 ppm, in the absence of Cd^{2+} ions) shifted toward a higher field. Important signals are labeled with their respective residue numbers.

namely GA10.[8] GA10*Sp*S can capture metal ions in the same manner as GA10. By contrast, the ^{1}H chemical shifts of GA10*Rp*S around the P9 phosphorothioate moiety were different from those of the parental GA10 in the absence of Cd^{2+} ions, suggesting that the introduction of a bulky sulfur atom at the P9 site had adversely affected the conformation. However, the shift of signals from GA10*Rp*S that was induced by Cd^{2+} ions was similar to that observed with GA10. Thus, the addition of Cd^{2+} ions caused a change in and a correction of conformation of GA10*Rp*S and the resultant, induced and "corrected" metal-binding form was identical to that of GA10. These result suggests that the introduction of a sulfur atom at the pro-*Rp* position of A9/G10.1 can change the conformation of the ribozyme and that this conformational change has a negative effect on the hammerhead reaction, whereas the corresponding replacement at the pro-*Sp* position does not influence the structure of the hammerhead ribozyme and does not affect the catalytic activity. Since the structure of a ribozyme with an *Rp*-phosphorothioate in the absence of thiophilic metal ions is different from that of the natural ribozyme in the absence of those thiophilic metal ions, reactions catalyzed by these two different ribozymes in the presence of only hard metal ions can be quite different from each other.

While, it is still generally accepted, on the basis of the first crystal structure and kinetic studies, that coordination of a metal ion at the A9 pro-*Rp* oxygen at A9/G10.1 is essential for hammerhead catalysis, our present analysis argues against the previous interpretation. Our data and previous structural and kinetic data can best be interpreted if we simply assume that the introduction of a sulfur atom at the *Rp*-position but not at the *Sp*-position deforms the active conformation of the ribozyme and that a Cd^{2+} ion can interact with either an *Rp*- or an *Sp*-phosphorothioate at the A9/G10.1 site to generate an active ribozyme. The reduced rate of cleavage by the *Rp*-phosphorothioate appeared to be due to the negative effects of the structural change that were induced by the sulfur atom of the *Rp*-phosphorothioate. Thus, care must be taken in the interpretation of thio-effects and Cd^{2+}-rescue effects in kinetic analyses.[1h,10]

Results

One-Dimensional (1D) ^{1}H and ^{31}P NMR and Two-Dimensional (2D) Natural-Abundance ^{1}H-^{13}C HSQC Spectroscopy. It has been reported that changes in chemical shifts of bases and phosphate groups provide evidence of the binding of metal ions and conformational changes.[8b,c,11] In this study, we examined chemical shifts in ^{1}H, ^{31}P, and ^{13}C NMR spectra in an effort to elucidate the structural changes in GA10*Sp*S and GA10*Rp*S that occur upon the addition of Cd^{2+} ions. The 1D ^{1}H and ^{31}P NMR spectra are shown in Figure 2 and Figure 3, respectively. It was impossible to detect signals from base carbons directly because of the low concentrations of our samples. We used natural abundance ^{1}H-^{13}C HSQC spectra

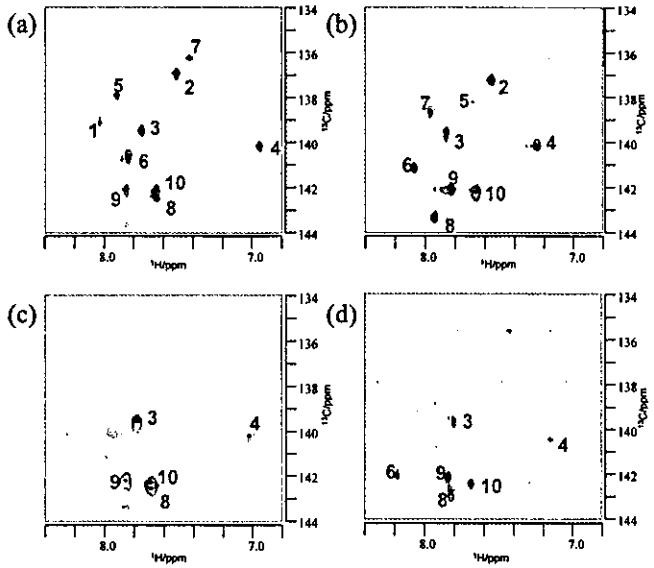

Figure 4. Natural-Abundance ^{1}H-^{13}C HSQC spectra of GA10*Sp*S in the absence of Cd^{2+} ions (a), of GA10*Sp*S in the presence of 1 molar equivalent of Cd^{2+} ions (b), of GA10*Rp*S in the absence of Cd^{2+} ions (c), and of GA10*Rp*S in the presence of 1 molar equivalent of Cd^{2+} ions (d). Intraresidue cross-peaks are labeled with their respective residue numbers.

for indirect detection of C6/C8 ^{13}C chemical shifts (Figure 1d and Figure 4).

The samples for NMR spectroscopy contained 1.77 mM GA10*Sp*S or 1.62 mM GA10*Rp*S as a duplex and 40 mM $NaClO_4$ at pH 7.6, plus $^{113}CdCl_2$, at various concentrations, namely, 0, 1.77 and 3.54 mM for GA10*Sp*S and 0, 1.62 and 3.24 mM for GA10*Rp*S. These concentrations of $CdCl_2$ corresponded to 0, 1 and 2 molar equivalents relative to GA10*Sp*S and GA10*Rp*S as a duplex. At each concentration of $CdCl_2$, we recorded the ^{1}H and ^{31}P NMR spectra and the ^{1}H-^{13}C HSQC spectra in D_2O at 40 °C.

Effects of the Sulfur Atom on the Structure of GA10*Sp*S and GA10*Rp*S in the Absence of Cd^{2+} ions. The signals due to the H6 and H8 protons of GA10*Sp*S and GA10*Rp*S in Figure 2 were assigned by reference to NOESY spectra. The H8 protons of G7 and G5 differed significantly between GA10*Sp*S and GA10*Rp*S. The chemical shift of the H8 proton of G7 (7.88 ppm) in GA10*Rp*S was significantly lower-field than that of GA10*Sp*S (7.42 ppm), suggesting a difference in conformation. The profile of the ^{31}P signals from GA10*Rp*S were broader than those from GA10*Sp*S. However, the ^{31}P chemical shifts for GA10*Sp*S and GA10*Rp*S were almost the same, as shown in Figure 3. Table 1 shows the assignments of ^{1}H and ^{31}P NMR signals in the absence of Cd^{2+} ions and the differences in chemical shifts relative to most of the parental GA10, which does not include a phosphorothioate moiety. The signals due to the protons of GA10*Sp*S were almost identical to those of GA10. The chemical shifts are different only by ±0.02 ppm.

The signals due to the protons of GA10*Rp*S were not the same as those of GA10. In particular, signals associated with C4, G5, A6, and G7 were very different from those of GA10. These results indicate that the effect of the sulfur atom on the structure of GA10*Sp*S was negligible but the effect of the sulfur atom on the structure of GA10*Rp*S was large, probably because the *Rp*-sulfur atom is located toward the inside in the major groove that is a crowded position. The inserted sulfur atom in GA10*Rp*S apparently changed the structure from that of the

Table 1. ^{1}H (H6/H8) and ^{31}P Chemical Shifts (ppm) of GA10*Sp*S and GA10*Rp*S at 40 °C in the Absence of Cd^{2+} Ions and Differences in Chemical Shifts from Those of GA10

	GA10*Sp*S				GA10*Rp*S			
	^{1}H (H6/H8)		^{31}P		^{1}H (H6/H8)		^{31}P	
base no.	ppm[a]	Δ[c]	ppm[b]	Δ[c]	ppm[a]	Δ[d]	ppm[b]	Δ[d]
1	8.02	0.01			8.02	0.01		
2	7.50	0.02	2.12	−0.08	7.62	0.14	2.23	0.03
3	7.73	−0.02	1.93	0	7.80	0.05	1.95[e]	0.02
4	6.94	−0.02	2.06	−0.03	7.07	0.11	1.95[e]	−0.14
5	7.90	0.01	1.46	−0.15	7.70	−0.19	1.66	0.05
6	7.83	−0.01	58.5	56.15	8.02	0.18	59.37	57.02
7	7.42	0	2.24	−0.03	7.88	0.46	2.23	−0.04
8	7.64	−0.02	1.22	0.06	7.70	0.04	1.16	0
9	7.85	0	1.66	−0.04	7.88	0.03	1.66[e]	−0.04
10	7.64	−0.01	1.62	−0.04	7.70	0.05	1.66[e]	0

[a] Relative to DSS. [b] Relative to 85% H_3PO_4. [c] The difference in chemical shifts (GA10*Sp*S−GA10). [d] The difference in chemical shifts (GA10*Rp*S−GA10). [e] Tentative assignment since the signal was broadening and no correlation could be obtained in the ^{1}H−^{31}P HMQC NOESY spectrum.

parental GA10. Although the only difference between GA10*Rp*S and GA10 is the replacement of an oxygen atom by a sulfur atom in the former at the pro-***Rp*** position of A6, the conformation of GA10*Rp*S was not identical to that of GA10. Although the H8 proton of G2 in GA10*Rp*S is away from the metal binding site, the thiolation affected the chemical shift of this proton more than that of C4 though the origin of this shift is unknown (Table 1). However, the chemical shifts of ^{31}P signals were almost the same for GA10*Rp*S and GA10, suggesting that the conformation of the backbone of GA10*Rp*S was almost identical to that of GA10.[12] Thus, the effect of the sulfur atom in GA10*Rp*S appeared to be local and limited to the region around the A6 position, which is considered to be the metal-binding site.

The ^{1}H-^{13}C HSQC spectrum (Figure 4) in the absence of Cd^{2+} ions was consistent with the results deduced from the 1D ^{1}H and ^{31}P spectra. The ^{1}H-^{13}C HSQC spectrum of GA10*Sp*S (Figure 4a) was almost identical to that of GA10,[8d] whereas the spectrum of GA10*Rp*S (Figure 4c) differed from that of GA10. The cross-peaks associated with G5, A6, and G7 were missing from the HSQC spectrum of GA10*Rp*S, suggesting that this metal-binding region around A6 might be associated with midrange chemical exchange on the NMR time-scale and might adopt multiple conformations locally. From the 1D ^{1}H and ^{31}P NMR spectra and the natural-abundance ^{1}H-^{13}C HSQC spectra, we deduced that the structure of GA10*Sp*S was almost identical to that of the parental and unmodified metal-binding motif, GA10, whereas the structure of GA10*Rp*S differed locally from the structure of GA10 around the metal-binding site in the absence of thiophilic Cd^{2+} ions. Furthermore, it appeared that midrange chemical exchange occurred around the metal-binding site of GA10*Rp*S.

(10) (a) Zhou, D. M.; Kumar, P. K. R.; Zhang L. H.; Taira K. *J. Am. Chem. Soc.* **1996**, *118*, 8969−8970. (b) Zhou, D. M.; Taira K. *Chem. Rev.* **1998**, *98*, 991−1026.
(11) (a) Wilson, W. D.; Heyl, B. L.; Reddy, R.; Marzilli, L. G. *Inorg. Chem.* **1982**, *21*, 2527−2528. (b) Pecoraro, V. L.; Hermes, J. D.; Cleland, W. W. *Biochemistry* **1984**, *23*, 5262−5271. (c) Jia, X.; Zon, G.; Marzilli, L. G. *Inorg. Chem.* **1991**, *30*, 228−239. (d) Mukundan, S., Jr.; Xu, Y.; Zon, G.; Marzilli, L. G. *J. Am. Chem. Soc.* **1991**, *113*, 3021−3027. (e) Legault, P.; Hoogstraten, C. G.; Metlitzky, E.; Pardi, A. *J. Mol. Biol.* **1998**, *284*, 325−335.
(12) Fürtig, B.; Richter, C.; Wöhnert, J.; Schwalbe, H. *ChemBioChem* **2003**, *4*, 936−962.

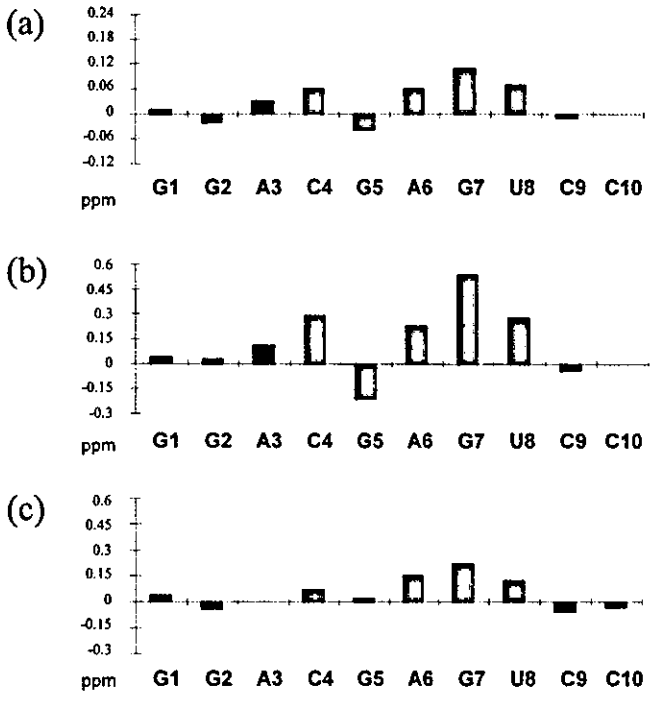

Figure 5. Changes in ^{1}H chemical shifts of H6/H8 protons of GA10 (a), GA10*Sp*S (b) and GA10*Rp*S (c) upon the addition of 1 molar equiv of Cd^{2+} ions.

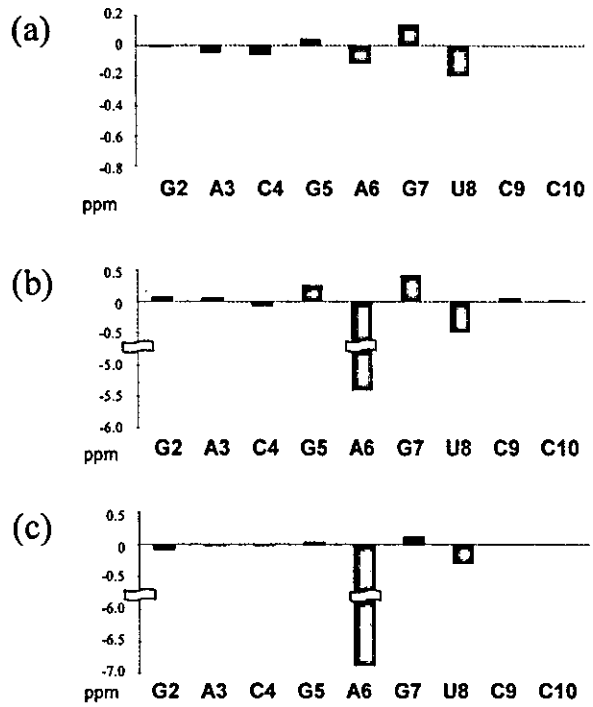

Figure 6. Changes in ^{31}P chemical shifts of phosphate signals of GA10 (a), GA10*Sp*S (b) and GA10*Rp*S (c) with the addition of one molar equiv of Cd^{2+} ions.

Perturbations Caused by Cd^{2+} Ions in GA10*Sp*S and GA10*Rp*S. The ^{1}H signals of GA10*Sp*S and GA10*Rp*S shifted upon the addition of Cd^{2+} ions (Figure 2). The changes of the chemical shifts are summarized in Figure 5 in a comparison with those for GA10. It should be noted that this decamer is self-complementary, thus, it contains two possible metal binding sites, and the addition of 1 molar equivalent Cd^{2+} will only occupy one site. However, because of the symmetry and fast-exchange, the observed ^{1}H NMR spectra for GA10*Sp*S and GA10*Rp*S were averaged singly metal-occupied structure. The changes in chemical shifts for GA10*Sp*S upon the addition of Cd^{2+} ions were similar to those for GA10. The proton signals associated with C4, A6, G7, and U8 moved largely downfield and the proton signal associated with G5 moved upfield upon the addition of Cd^{2+} ions to GA10*Sp*S (Figure 5b). These changes were almost identical to those of GA10 (Figure 5a). The signals for GA10*Sp*S were almost identical to those of GA10 not only in the absence of Cd^{2+} ions but also in the presence of Cd^{2+}, suggesting that these two motifs had similar conformations despite the introduction of a bulky sulfur atom at the *Sp*-position of the P9 phosphate in GA10*Sp*S.

Although the movements of signals were not as large as those of signals from GA10*Sp*S, the actual number of shifted signals from GA10*Rp*S was similar to the number from GA10 (Figure 5c), suggesting that metal coordination occurred around the same region of GA10. Moreover, the proton signals associated with C4, A6, G7, and U8 also moved downfield. Thus, we can conclude, from the movement of ^{1}H signals, that the final form of GA10*Rp*S with bound metal ions was similar to that of GA10 with bound metal ions. In other words, although the conformation of GA10*Rp*S in the absence of Cd^{2+} ions was different from that of GA10, the added Cd^{2+} ions were able to induce a conformational change in GA10*Rp*S such that it adopted a conformation similar to that of GA10 with bound Cd^{2+} ions. Note that the vertical scales for GA10*Sp*S and GA10*Rp*S in Figure 5 are different from that for GA10. The changes in chemical shifts of GA10*Sp*S and GA10*Rp*S in ^{1}H NMR spectra were larger than those of GA10. The larger size of the changes in chemical shifts of GA10*Sp*S and GA10*Rp*S that were induced by the sulfur atom and Cd^{2+} ions can be explained by the *H*ard and *S*oft *A*cid *B*ase (HSAB) rule.[13] Thus, a 'soft acid', such as a Cd^{2+} ion, prefers to bind to a sulfur atom, which is a 'soft base' (within GA10*Sp*S and GA10*Rp*S) than to an oxygen atom, which is a 'hard base' (within GA10).

Figure 6 shows the changes in ^{31}P chemical shifts of signals from GA10*Sp*S and GA10*Rp*S upon the addition of Cd^{2+} ions, in a comparison with GA10. The changes in signals for GA10*Sp*S (Figure 6b) and GA10*Rp*S (Figure 6c) were similar to those for GA10 (Figure 6a). Since the sulfur atom of the phosphorothioate moiety binds more tightly to a Cd^{2+} ion than does an oxygen atom, the signals associated with A6 within GA10*Sp*S and GA10*Rp*S moved largely upfield. The shifts in the ^{31}P signal of the phosphorothioate were 5.4 and 6.87 ppm for GA10*Sp*S and GA10*Rp*S, respectively, upon the addition of 1 molar equiv of Cd^{2+} ions. The ^{31}P signals associated with G5 and G7 moved downfield and those of U8 moved upfield in all these oligomers. The directions of the movements of these respective signals from GA10*Sp*S and GA10*Rp*S were identical to those from GA10, indicating that the structures of GA10*Sp*S and GA10*Rp*S were changed by binding of Cd^{2+} ions and that the metal-bound forms of GA10*Sp*S and GA10*Rp*S were similar to that of GA10.[12]

The changes in ^{13}C chemical shifts for GA10*Sp*S also resembled those for GA10 (Figure 4).[8b] The cross-peaks associated with G5, A6, G7, and U8 moved considerably and the directions of movements of respective cross-peaks were identical to those for GA10 (Figure 4, parts a and b). In the

(13) (a) Pearson, R. G. *J. Chem. Educ.* **1968**, *45*, 581–587. (b) Pearson, R. G. *J. Chem. Educ.* **1968**, *45*, 643–648.

case of GA10*R*pS, although cross-peaks associated with G5 and G7 were not detected, the cross-peak associated with A6 emerged upon the addition of Cd^{2+} ions (Figure 4, parts c and d). The cross-peak associated with U8 in GA10*R*pS shifted in the same direction as that in GA10. It appeared, from our analysis of the movements of ^{1}H, ^{31}P and ^{13}C resonances, that the structural changes in GA10*S*pS and GA10*R*pS that accompany coordination of a thiophilic metal ion resemble to those in GA10 and lead, eventually, to the similar active form upon the addition of appropriate metal ions.

Discussion

In this report, we described the characterization of the metal-binding forms of GA10*S*pS and GA10*R*pS, which correspond to the metal-binding motif of the A9/G10.1 site in a hammerhead ribozyme, by monitoring ^{1}H, ^{31}P, and ^{13}C NMR signals. GA10*S*pS and GA10*R*pS contained a phosphorothioate moiety at A6, which correspond to A9 in a hammerhead ribozyme and appear to be a metal-binding site. The ^{1}H and ^{13}C resonances of H6/H8 and C6/C8 atoms provided information about local structural changes around the A6 metal-binding sites of GA10*S*pS and GA10*R*pS. Comparisons of changes in chemical shifts with and without a sulfur atom at the A9/G10.1 site revealed the positional effect of the sulfur atom at P9 and the role of the pro-*S*p oxygen and the pro-*R*p oxygen at the A9/G10.1 site of hammerhead ribozymes.

Conformation of GA10*S*pS and GA10*R*pS in the Absence of Cd^{2+} Ions: The Effects of a Sulfur Atom at the pro-*R*p and pro-*S*p Positions on Structure. The effects of a sulfur atom on structure differed between GA10*S*pS and GA10*R*pS. The chemical shifts of the ^{1}H, ^{13}C, and ^{31}P signals of GA10*S*pS were almost identical to those of GA10 (Figure 2a, 3a, 4a, and Table 1). These results imply that the tertiary structures of GA10*S*pS and GA10 are similar and that the sulfur atom in GA10*S*pS does not induce a structural change. By contrast to those of GA10*S*pS, the ^{1}H and ^{13}C signals of GA10*R*pS were different from those of GA10 in the absence of Cd^{2+} ions (Figure 2b, 4c, and Table 1). Although the line shape of ^{31}P signals from GA10*R*pS was broadened (Figure 3, parts c and d), the chemical shifts were similar to those of signals from GA10 except at position 6, which corresponded to the phosphorothioate linkage (Table 1). Therefore, the results indicate that the sulfur atom of GA10*R*pS induced a conformational change around the metal-binding site of A6 but the backbone structure of GA10*R*pS was unaffected.[12] The radius of a sulfur atom is 1.85 Å and is 0.45 Å larger than that of an oxygen atom. The length of a P−S bond is 1.8 Å and is 0.3 Å longer than that of a P−O bond. Moreover, the pro-*R*p oxygen is located toward the inside in the major groove in the crystal structure and this location might not allow for any steric hindrance in the ribozyme's structure. The larger-radius sulfur atom, the longer P−S bond and the resultant steric hindrance by the pro-*R*p sulfur are likely to have induced a conformational change around the P9 metal-binding site and to have had a negative effect on the conformation of the ribozyme.

Binding of Metal Ions to GA10*S*pS and GA10*R*pS. In the previous study using a full-length hammerhead ribozyme, ^{31}P NMR signals of both *R*p- and *S*p-phosphorothioates shifted 2-3 ppm upfield upon the addition of 1 to 2 molar equiv of Cd^{2+} ions.[6] Similar changes were observed for the metal-binding motifs consisting solely of short GA10*S*pS and GA10*R*pS, although the magnitude of the upfield shift (5-7 ppm) upon addition of 1 equiv of Cd^{2+} was greater for the short oligomers probably because the full-length ribozyme might have more nonspecific interactions and/or specific interactions at site(s) other than the A9/G10.1 site between phosphates and Cd^{2+} ion-(s) that had increased the end-point by Cd^{2+} saturation. Nevertheless, since a Cd^{2+} ion can interact with *R*p- and *S*p-phosphorothioates in the metal-binding motif of both the full-length ribozyme and the shortened GA10*S*pS and GA10*R*pS and since complete assignments of ^{1}H, ^{13}C and ^{31}P signals were possible only for the short oligos, we in this study used GA10*S*pS and GA10*R*pS. Indeed, perturbations occurred not only in the ^{31}P signal from the inserted phosphorothioate (A6) but also in most of the ^{1}H, ^{13}C and ^{31}P signals, suggesting that there might have been a conformational change in both GA10*S*pS and GA10*R*pS as a result of the binding of Cd^{2+} ions. The perturbations in signals from GA10*S*pS were almost identical to those from GA10. Thus, the Cd^{2+}-binding form in GA10*S*pS was similar to that of GA10. In GA10*R*pS, even though the chemical shifts in the ^{1}H NMR spectrum in the absence of metal ions, in particular at the H6 and H8 positions, were different from those in GA10, the perturbations induced by Cd^{2+} ions resembled the perturbations induced by Cd^{2+} ions in GA10 (Figures 5 and 6). It is noteworthy that the conformation not only of GA10*S*pS with a bound metal ion but also of GA10*R*pS with a bound metal ion was similar to that of GA10 with a bound metal ion, even though, in the absence of metal ions, the conformation of GA10*R*pS was different from that of GA10.

Does a metal ion bind directly or indirectly to N7 and the phosphate oxygen at the A9/G10.1 metal-binding site? In a previous study, using ^{15}N-labeled GA10, we did not detect any coupling between the N7 atom at G7 and $^{113}Cd^{2+}$, even though signal perturbation occurred at this N7 atom and the C8 atom of G7.[8c] The binding of metal ions by GA10*S*pS and GA10*R*pS was stronger than that by GA10 because the phosphorothioate moiety contained a sulfur atom at the metal-binding site. The HSAB rule determines that a 'hard acid', such as a Mg^{2+} ion, prefers to bind to an oxygen atom. Before the titration of the phosphorothioate with Cd^{2+} ions, we expected that coupling might be evident, in the ^{31}P signal of A6 and the H8/C8 cross-peak of G7 in the ^{1}H-^{13}C HSQC spectra of GA10*R*pS and GA10*S*pS in the presence of one molar equivalent of Cd^{2+} ions, assuming that binding of metal ions would involve direct coordination.[14] No coupling between ^{31}P of A6 and ^{113}Cd (Figure 3, parts a and c) or between the H8 atom of G7 and ^{113}Cd (Figure 2, parts a and b) was detected in this study, even though large perturbations in chemical shifts were noted in the ^{31}P and ^{1}H NMR spectra.

Theoretical calculations of spin coupling constants and chemical shifts related to the binding of a divalent metal ion to guanine were reported recently.[15] The calculated chemical shift of the N7 atom of guanine for an inner-shell binding complex of Mg^{2+} ion with guanine is similar to the chemical shift detected experimentally by our group.[8d] The theoretical calcula-

(14) Damblon, C.; Prosperi, C.; Lian, L.-Y.; Barsukov, I.; Soto, R. P.; Galleni, M.; Frere, J.-M.; Roberts, G. C. K. *J. Am. Chem. Soc.* **1999**, *121*, 11575−11576.
(15) Sychrovsky, V.; Sponer, J.; Hobza, P. *J. Am. Chem. Soc.* **2004**, *126*, 663−672.

tions supported the direct coordination of a metal ion to the N7 atom of guanine,[15] suggesting the same conclusion as the one that we had reached on the basis of our experiments.[8d] The theoretical calculations, indicated that the change in chemical shift of the signal due to the C8 atom of G7 in the ^{1}H-^{13}C HSQC spectrum of GA10*Sp*S (Figure 4, parts a and b) implies the direct coordination of a Cd^{2+} ion to the N7 atom of G7,[15] although outer-sphere coordination cannot completely be ignored.[16] The coupling was absent in the present study, in which we used a sulfur atom and ^{113}Cd ions, because of rapid exchange of Cd^{2+} ions at the metal-binding site, although we cannot completely exclude the possibility of coupling between $^{113}Cd^{2+}$ and H8 of G7 in the case of the full length hammerhead ribozyme.

Pro-*Rp* Phosphorothioate at A9 of a Hammerhead Ribozyme. Kinetic studies of constructs with a phosphorothioate moiety at the A9/G10.1 site of hammerhead ribozymes suggested the important metal-binding role of the pro-***Rp*** oxygen but not of the pro-***Sp*** oxygen since the pro-***Rp*** sulfur-substituted ribozyme was inactive in Mg^{2+}-mediated reactions but was rescued by the addition of thiophilic Cd^{2+} ions. The corresponding pro-***Sp*** sulfur-substituted ribozyme was active even in Mg^{2+}-mediated reactions. However, this interpretation requires the assumption that the sulfur atom of the phosphorothioate does not affect the initial conformation of the hammerhead ribozyme, nor the corresponding structures in the presence of hard Mg^{2+} ions. If the inserted sulfur atom were to influence the conformation of the hammerhead ribozyme, then we would have to consider the effects of this conformation change in our interpretation of the kinetic results obtained with the phosphorothioate. In other words, the conformational change caused by insertion of sulfur might disrupt the ribozyme reaction if the conformation of the phosphorothioate-containing ribozyme is not an active conformation.

We demonstrated in the present study that, in the absence of metal ions, a conformational change does indeed occur as a result of the sulfur in GA10***Rp***S but it does not occur in GA10***Sp***S. Therefore, we can postulate that the conformation of the hammerhead ribozyme that contains a phosphorothioate moiety at the pro-***Rp*** of A9 is likely to be different from that of the wild-type ribozyme, whereas the hammerhead ribozyme that contains a phosphorothioate moiety at the pro-***Sp*** of A9 retains the conformation of the wild-type ribozyme. The decreased rate of the reaction catalyzed by the ribozyme that contains a phosphorothioate moiety at the pro-***Rp*** site means that the conformational change induced by the phosphorothioate has a negative effect on the ribozyme reaction. It appears that the rescue by Cd^{2+} ions in kinetic studies is due to the recovery of an active metal-associated form that resembles the metal-associated form of the wild-type ribozyme (remember that the changes in chemical shifts induced by Cd^{2+} ions in GA10***Rp***S were similar to those induced by Cd^{2+} ions in GA10).

In summary, we examined conformational changes upon the interaction of Cd^{2+} ions with the A9/G10.1 metal-binding motif of a hammerhead ribozyme. Our analysis demonstrated that the effects of the introduction of a phosphorothioate linkage at a specific position depend on whether the sulfur is at the pro-***Rp*** or the pro-***Sp*** position. Since the effects at the two positions are not the same, the resultant conformers are likely to be at different energy levels or, in catalytic nucleic acids, they are likely to have different activities, a possibility that has been ignored in the past. Indeed, two observations can be most simply and best explained by this conclusion. The first of these two observations is that the pro-***Rp*** sulfur-substituted ribozyme is inactive in Mg^{2+}-mediated reactions but its activity can be rescued by the addition of thiophilic Cd^{2+} ions, whereas the corresponding pro-***Sp*** sulfur-substituted ribozyme is active even in Mg^{2+}-mediated reactions. The second observation is that the conformation of GA10***Sp***S is similar to that of the parental GA10, whereas the conformation of GA10***Rp***S is different from that of the parental GA10 in the absence of Cd^{2+} ions, even though all oligomers yield similar Cd^{2+}-bound forms. Thus, the introduction of sulfur at the pro-***Rp*** position but not at the pro-***Sp*** position disturbs the active conformation of the ribozyme. Our analysis clearly warns against incautious interpretations of thio-effects and rescue phenomena because the previous assumption that the two different conformers have the same effects, other than the effects of position, is clearly not always valid.

Experimental Section

Preparation of Samples. A crude mixture of the GA10***Rp***S and GA10***Sp***S phosphorothioate isomers was purchased from Genset Corporation (France). The two components of the mixture were separated and purified as described previously.[7] Assignments of isomers were made after digestion by snake venom phosphodiesterase and nuclease P1.[17] For digestion by snake venom phosphodiesterase, an aliquot of each thio-substituted oligonucleotide (0.5 nmol) was incubated for 8 h at 37 °C with snake venom phosphodiesterase (0.1 μg; Sigma-Aldrich, USA) and calf alkaline phosphatase (6.0 μg; Takara, Japan) in 0.05 M Tris-HCl (pH 9.0), 0.3 mM DTT and 1 mM $MgCl_2$ in a total volume of 150 μL. The products were analyzed directly by HPLC on a reversed-phase column (TSK-GEL ODS-80TM; length, 250 mm; i.d., 4.6 mm; Tosoh, Japan) with a gradient of buffer A, namely, 0.1 M triethylammonium acetate (pH 7.0), and buffer B, which consisted of 60% buffer A and 40% acetonitrile (5% B for 15 min followed by 5% to 100% B over the course of 45 min). Retention times under these conditions were as follows: cytidine, 2.86 min; uridine, 5.89 min; guanosine, 8.02 min; and adenosine, 12.31 min. The products of digestion of the later-eluting isomer generated a peak at 25.87 min that corresponded to ***Sp***-GpsA. For digestion by nuclease P1, an aliquot of each thio-substituted oligonucleotide (0.5 nmol) was digested with nuclease P1 (2.0 μg; Sigma-Aldrich) in distilled water (120 μL) for 1 h at 37 °C. The solution was buffered with 16 μL of 50 mM Tris-HCl (pH 9.0) and digested with calf alkaline phosphatase (6.0 μg; Takara) for 1 h at 37 °C. The products were analyzed by reversed-phase HPLC as described above. The products of digestion of the earlier-eluting isomer generated a peak at 24.46 min that corresponded to ***Rp***-GpsA.

Resonance Assignments. Samples for NMR spectroscopy were prepared by dissolving purified oligomers in 60 μL of a

(16) Wang, G.; Gaffney, B. L.; Jones, R. A. *J. Am. Chem. Soc.* **2004**, *126*, 8908–8909.

(17) (a) Burgers, P. M.; Eckstein, F. *Biochemistry* **1979**, *18*, 592–596. (b) Almer, H.; Stawinski, J.; Strömberg, R. *J. Chem. Soc., Chem. Commun.* 1994, 1459–1460. (c) Stec, W. J.; Zon, G.; Egan, W.; Stec, B. *J. Am. Chem. Soc.* **1984**, *106*, 6077–6079. (d) Connolly, B. A.; Potter, B. V. L.; Eckstein, F.; Pingoud, A.; Grotjahn, L. *Biochemistry* **1984**, *23*, 3443–3453.

solution, prepared in D_2O, of 40 mM $NaClO_4$ and 10 mM sodium cacodylate buffer at pH 7.6 in a 3-mm NMR tube (Shigemi, Japan). The concentrations of GA10*S*pS and GA10*R*pS, each as a duplex were 1.77 mM and 1.62 mM, respectively. Concentrated solutions of $CdCl_2$ were added directly to each sample to give desired concentration. All NMR spectra were acquired on an INOVA 600 MHz NMR spectrometer (Varian, USA) operated at 40 °C, with a *z*-axis pulsed-field gradient probe. The chemical shifts of protons were determined relative to the signal from the internal standard, sodium 4,4-dimethyl-4-silapentane-1-sulfonate (DSS). The ^{31}P chemical shifts were referenced to an external 85% solution of H_3PO_4. Aromatic ^1H and ^{13}C resonances were assigned from ^1H-^1H NOESY, natural-abundance ^1H-^{13}C HSQC and ^1H-^{31}P HMQC NOESY spectra. Typical ^1H-^1H NOESY spectra were recorded with 4096 × 1024 complex points for a spectral width of 5071.0 Hz; 64 scans were averaged; and the mixing time was 300 ms. Natural-abundance ^1H-^{13}C HSQC spectra were recorded with 2048 × 160 complex points for a spectral width of 4743.8 × 6034.1 Hz, and 1408 scans were averaged. 2D ^1H-^{31}P HMQC NOESY spectra were recorded with 2048 × 32 complex points for a spectral width of 4821.6 × 1457.1 Hz; 2048 scans were averaged; and the mixing time for NOESY was 300 ms.

Acknowledgment. The authors thank Dr. Tanaka at Tohoku University and Dr. Furihata at Tokyo University for their helpful comments.

JA0472937

J|A|C|S
ARTICLES
Published on Web 09/11/2004

Analysis on a Cooperative Pathway Involving Multiple Cations in Hammerhead Reactions

Yasuomi Takagi,[†,‡] Atsushi Inoue,[†,§] and Kazunari Taira*[,†,§]

Contribution from the Gene Function Research Center, National Institute of Advanced Industrial Science and Technology (AIST), Central 4, 1-1-1 Higashi, Tsukuba Science City, 305-8562, Japan, iGENE Therapeutics, Inc., c/o AIST, Central 4, 1-1-1 Higashi, Tsukuba Science City, 305-8562, Japan, and Department of Chemistry and Biotechnology, School of Engineering, The University of Tokyo, Hongo, Tokyo 113-8656, Japan

Received December 29, 2003; E-mail: taira@chembio.t.u-tokyo.ac.jp

Abstract: The hammerhead ribozyme reaction is more complex than might have been expected, perhaps because of the flexibility of RNA, which would have enhanced the potential of RNA during evolution of and in the RNA world. Divalent Mg^{2+} ions can increase the rate of the ribozyme-catalyzed reaction by approximately 10^9-fold as compared to the background rate under standard conditions. However, the role of Mg^{2+} ions is controversial since the reaction can proceed in the presence of high concentrations of monovalent ions, such as Li^+, Na^+, and NH_4^+ ions, in the absence of divalent ions. We thus carried out ribozyme reactions under various conditions, and we obtained parameters that explain the experimental data. On the basis of the analysis, we propose a new pathway in the hammerhead ribozyme reaction in which divalent metal ions and monovalent ions act cooperatively.

Introduction

Catalytic RNAs that are found in nature include hammerhead, hairpin, hepatitis delta virus (HDV), and Varkud satellite (VS) ribozymes; Group I and II introns; and the RNA subunit of RNase P.[1-13] Furthermore, structural and chemical analyses strongly suggest that ribosomal RNA is a ribozyme,[14-18] and the possibility exists that the RNA component of the spliceosome might also be a ribozyme.[19] Early research on ribozymes suggested that all ribozymes might be metalloenzymes that require divalent metal ions, in particular Mg^{2+} ions, for catalysis, and that all might operate by a basically similar mechanism. However, extensive subsequent studies revealed that the catalytic activity of hairpin ribozymes is independent of divalent metal ions.[20-26] Although Group I and II introns and the RNA subunit of RNase P apparently exploit several divalent metal ions as catalysts,[27-34] the HDV ribozyme uses a combination of a divalent metal ion and a nucleobase,[35] while hairpin ribozymes seem to use a nucleobase only.[26] It has been suggested that ribosomal RNA also makes use of a nucleobase in the peptidyl transferase reaction rather than a divalent metal ion.[15-17] Thus, the various types of ribozyme appear to exploit different cleavage mechanisms, which depend, in turn, upon the architecture of each individual ribozyme.[36] Even hammerhead

† Gene Function Research Center, AIST.
‡ iGENE Therapeutics, Inc.
§ The University of Tokyo.

(1) Cech, T. R.; Zaug, A. J.; Grabowski, P. J. *Cell* **1981**, *27*, 487−496.
(2) Guerrier-Takada, C.; Gardiner, K.; Marsh, T.; Pace, N.; Altman, S. *Cell* **1983**, *35*, 849−857.
(3) Michel, F.; Umesono, K.; Ozeki, H. *Gene* **1989**, *82*, 5−30.
(4) Foster, A. C.; Symons, R. H. *Cell* **1987**, *50*, 9−16.
(5) Buzayan, J. M.; Gerlach, W. L.; Bruening, G. *Nature* **1986**, *323*, 349−353.
(6) Carola, C.; Eckstein, F. *Curr. Opin. Chem. Biol.* **1999**, *3*, 274−283.
(7) Hampel, A.; Tritz, R.; Hicks, M.; Cruz, P. *Nucleic Acids Res.* **1990**, *18*, 299−304.
(8) Feldstein, P. A.; Bruening, G. *Nucleic Acids Res.* **1993**, *21*, 1991−1998.
(9) Sharmeen, L.; Kuo, M. Y.-P.; Dinter-Gottlieb, G.; Taylor, J. *J. Virol.* **1988**, *62*, 2674−2679.
(10) Kuo, M. Y.-P.; Sharmeen, L.; Dinter-Gottlieb, G.; Taylor, J. *J. Virol.* **1988**, *62*, 4439−4444.
(11) Perrotta, A. T.; Been, M. D. *Nature* **1991**, *350*, 434−436.
(12) Lai, M. M. *Annu. Rev. Biochem.* **1995**, *64*, 259−286.
(13) Collins, R. A.; Seville, B. J. *Nature* **1990**, *345*, 177−179.
(14) Noller, H. F.; Hoffarth, V.; Zimniak, L. *Science* **1992**, *256*, 1416−1419.
(15) Nissen, P.; Hansen, J.; Ban, N.; Moore; P. B.; Steitz, T. A. *Science* **2000**, *289*, 920−930.
(16) Muth, G. W.; Ortoleva-Donnelly, L.; Strobel, S. A. *Science* **2000**, *289*, 947−950.
(17) Bayfield, M. A.; Dahlberg, A. E.; Schulmeister, U.; Dorner, S.; Barta, A. *Proc. Natl. Acad. Sci. U.S.A.* **2000**, *98*, 10096−10101.
(18) Cech, T. R. *Science* **2000**, *289*, 878−879.
(19) Collins, C. A.; Guthrie, C. *Nat. Struct. Biol.* **2000**, *10*, 850−854.
(20) Hampel, A.; Cowan, J. A. *Chem. Biol.* **1997**, *4*, 513−517.
(21) Nesbitt, S.; Hegg, L. A.; Fedor, M. J. *Chem. Biol.* **1997**, *4*, 619−630.
(22) Young, K. J.; Gill, F.; Grasby, J. A. *Nucleic Acids Res.* **1997**, *25*, 3760−3766.
(23) Chowrira, B. M.; Berzal-Herranz, A.; Burke, J. M. *Biochemistry* **1993**, *32*, 1088−1095.
(24) Earnshaw, D. J.; Gait, M. J. *Nucleic Acids Res.* **1998**, *26*, 5551−5561.
(25) Seyhan, A. A.; Burke, J. M. *RNA* **2000**, *6*, 189−198.
(26) Murray, J. B.; Seyhan, A. A.; Walter, N. G.; Burke, J. M.; Scott, W. G. *Chem. Biol.* **1998**, *5*, 587−595.
(27) Shan, S.; Yoshida, A.; Sun, S.; Piccirilli, J. A.; Herschlag, D. *Proc. Natl. Acad. Sci. U.S.A.* **1999**, *96*, 12299−12304.
(28) Yoshida, A.; Sun, S.; Piccirilli, J. A. *Nat. Struct. Biol.* **1999**, *6*, 318−321.
(29) Shan, S.; Kravchuk, A. V.; Piccirilli, J. A.; Herschlag, D. *Biochemistry* **2001**, *40*, 5161−5171.
(30) Gordon, P. M.; Sontheimer, E. J.; Piccirilli, J. A. *RNA* **2000**, *6*, 199−205.
(31) Gordon, P. M.; Sontheimer, E. J.; Piccirilli, J. A. *Biochemistry* **2000**, *39*, 12939−12952.
(32) Kurz, J. C.; Fierke, C. A. *Curr. Opin. Chem. Biol.* **2000**, *4*, 553−558.
(33) Warnecke, J. M.; Held, R.; Busch, S.; Hartmann, R. K. *J. Mol. Biol.* **1999**, *290*, 433−445.
(34) Pfeiffer, T.; Tekos, A.; Warnecke, J. M.; Drainas, D.; Engelke, D. R.; Seraphin, B.; Hartmann, R. K. *J. Mol. Biol.* **2000**, *298*, 559−565.
(35) Nakano, S.; Proctor, D. J.; Bevilacqua, P. C. *Biochemistry* **2001**, *40*, 12022−12038.
(36) Takagi, Y.; Warashina, M.; Stec, W. J.; Yoshinari, K.; Taira, K. *Nucleic Acids Res.* **2001**, *29*, 1815−1834.

10.1021/ja031991u CCC: $27.50

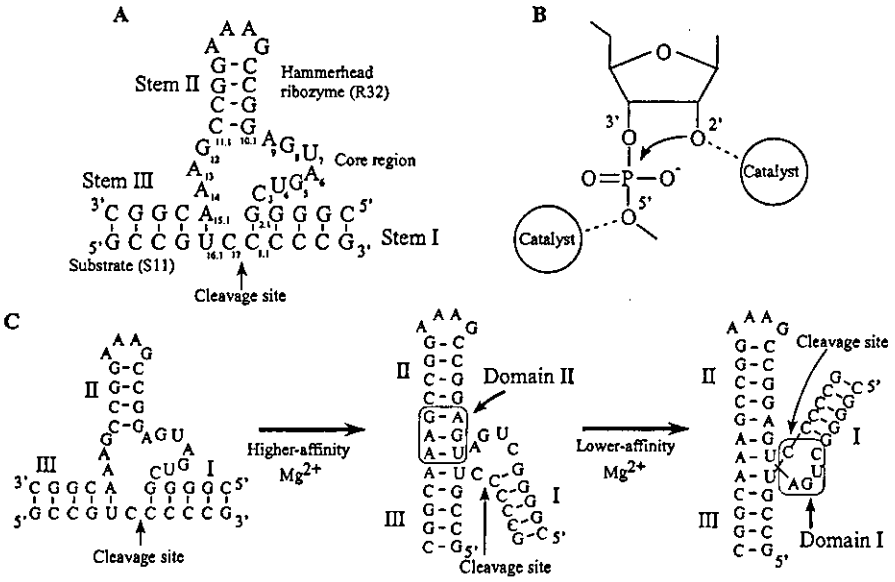

Figure 1. (A) Sequence and secondary structure of the hammerhead ribozyme (R32) and the substrate (S11) used in this study. (B) Schematic representation of the proposed mechanism of the hammerhead ribozyme reaction. The 2′-hydroxyl moiety is activated by the catalyst and then launches a nucleophilic attack on the adjacent phosphate, with subsequent cleavage of the bond at the 5′-oxygen. The developing negative charge on the leaving 5′-oxygen is stabilized by another catalyst. (C) Proposed two-stage scheme for folding of the ribozyme−substrate complex. The higher-affinity Mg^{2+} ion(s) drives the formation of domain II, which includes non-Watson−Crick base pairs, and the lower-affinity Mg^{2+} ion(s) rotates around helix I, forming the catalytic core.

ribozymes, which have generally been characterized as typical metalloenzymes, can no longer be categorized unambiguously.[26,36−38]

Hammerhead ribozymes, which act *in cis* during viral replication by the rolling circle mechanism, were identified originally in certain RNA viruses.[39] In the laboratory, ribozymes have been engineered such that they act on other RNA molecules *in trans* and catalyze the cleavage of phosphodiester bonds at specific sites to generate specific products, each of which has a 2′,3′-cyclic phosphate and a 5′-hydroxyl group (Figure 1A).[40−43] The transesterification reaction includes deprotonation of the 2′-hydroxyl moiety of a ribose group, nucleophilic attack of the 2′-oxygen on the adjacent phosphorus atom, and stabilization (neutralization) of the 5′-oxyanion leaving group (Figure 1B).[44] A large body of evidence also indicates that the $P9/G_{10.1}$ site binds a metal ion with high affinity, with other metal ion-binding sites being located around the G_5 nucleobase and the A_{13} phosphate near the site of cleavage.[45−48] Thus, the idea that ribozymes are metalloenzymes has become generally accepted. However, it was reported recently that ribozymes are active in the presence of very high concentrations of monovalent cations, such as Li^+ or NH_4^+ ions, or at moderate (below 100 mM) concentrations of the exchange-inert complex ion $Co(NH_3)_6^{3+}$, in the absence of divalent metal ions.[26,37] These findings raise the possibility that it might be inappropriate to classify hammerhead ribozymes as metalloenzymes. By contrast, we observed a difference in numbers of protons transferred in the transition state between ribozyme-catalyzed reactions that were allowed to proceed in the presence of Mg^{2+}, Li^+, and NH_4^+ ions, and we proposed that the catalyst in the reaction might depend on the conditions of the reaction.[36,49−51]

Our previous kinetic analysis supported the "two-phase folding model" that was originally proposed by Lilley and coworkers (Figure 1C).[50,52−56] In this study, we examined the validity of the two-phase folding model and the reaction pathway by performing stoichiometric analyses of our hammerhead ribozyme's activity as a function of the concentration of different monovalent ions in the presence and in the absence of Mg^{2+} ions. Our results strongly support the existence of the novel cooperative pathway in the hammerhead ribozyme reaction. We also found that our hammerhead ribozyme has a very unique characteristic with respect to the dependence of its reaction on Mg^{2+} ions, even in the presence of approximately 1 M Mg^{2+} ions. Such dependence suggests that the ribozyme's activity

(37) Curtis, E. A.; Bartel, D. P. *RNA* **2001**, *7*, 546−552.
(38) O'Rear, J. L.; Wang, S.; Feig, A. L.; Beigelman, L.; Uhlenbeck, O. C.; Herschlag, D. *RNA* **2001**, *7*, 537−545.
(39) Symons, R. H. *Annu. Rev. Biochem.* **1992**, *61*, 641−671.
(40) Uhlenbeck, O. C. *Nature* **1987**, *328*, 596−600.
(41) Haseloff, J.; Gerlach, W. L. *Nature* **1988**, *334*, 585−591.
(42) Hutchins, C. J.; Rathjen, P. D.; Forster, A. C.; Symons, R. H. *Nucleic Acids Res.* **1986**, *14*, 3627−3640.
(43) Koizumi, M.; Hayase, Y.; Iwai, S.; Kamiya, H.; Inoue, H.; Ohtsuka, E. *Nucleic Acids Res.* **1989**, *17*, 7059−7071.
(44) Zhou, D.-M.; Taira, K. *Chem. Rev.* **1998**, *98*, 991−1026.
(45) Wang, S.; Karbstein, K.; Peracchi, A.; Beigelman, L.; Herschlag, D. *Biochemistry* **1999**, *38*, 14363−14378.
(46) Maderia, M.; Hunsicker, L. M.; DeRose, V. J. *Biochemistry* **2000**, *39*, 12113−12120.
(47) (a) Zhou D.-M.; Kumar, P. K. R.; Zhang, L.-H.; Taira, K. *J. Am. Chem. Soc.* **1996**, *118*, 8969−8970. (b) Yoshinari, K.; Taira. K. *Nucleic Acids Res.* **2000**, *28*, 1730−1742. (c) Suzumura, K.; Yoshinari, K.; Tanaka, Y.; Takagi, Y.; Kasai, Y.; Warashina, M.; Kuwabara, T.; Orita, M.; Taira, K. *J. Am. Chem. Soc.* **2002**, *124*, 8230−8236. (d) Warashina, M.; Kuwabara, T.; Nakamatsu, Y.; Takagi, Y.; Kato, Y.; Taira, K. *J. Am. Chem. Soc.* **2004**, *126*, XXXX−XXXX.
(48) Peracchi, A.; Beigelman, L.; Scott, E. C.; Uhlenbeck, O. C.; Herschlag, D. *J. Biol. Chem.* **1997**, *272*, 26822−26826.
(49) Sawata, S.; Komiyama, M.; Taira, K. *J. Am. Chem. Soc.* **1995**, *117*, 2357−2358.
(50) (a) Zhou, J.-M.; Zhou, D.-M.; Takagi, Y.; Kasai, Y.; Inoue, A.; Baba, T.; Taira, K. *Nucleic Acids Res.* **2002**, *30*, 2374−2382. (b) Inoue, A.; Takagi, Y.; Taira, K. *Nucleic Acids Res.* **2004**, *32*, 4217−4223. (c) Takagi, Y.; Ikeda, Y.; Taira, K. *Topics Curr. Chem.* **2004**, *232*, 213−251.
(51) Takagi, Y.; Taira, K. *J. Am. Chem. Soc.* **2002**, *124*, 3850−3852.
(52) Bassi, G. S.; Murchie, A. I. H.; Walter, F.; Clegg, R. M.; Lilley, D. M. J. *EMBO J.* **1997**, *16*, 7481−7489.
(53) Horton, T. E.; Clardy, D. R.; DeRose, V. J. *Biochemistry* **1998**, *37*, 18094−18101.
(54) Bassi, G. S.; Møllegaard, N. E.; Murchie, A. I. H.; Lilley. D. M. J. *Biochemistry* **1999**, *38*, 3345−3354.
(55) Hammann, C.; Norman, D. G.; Lilley, D. M. J. *Proc. Natl. Acad. Sci. U.S.A.* **2001**, *98*, 5503−5508.
(56) Bassi, G. S.; Møllegaard, N. E.; Murchie, A. I. H.; von Kitzing, E.; Lilley, D. M. J. *Nat. Struct. Biol.* **1995**, *2*, 45−55.

reaches more than 100 min^{-1} at pH 8 and 25 °C in the presence of more than 800 mM Mg^{2+} ions. Our ribozyme might, thus, be very suitable for studies of the mechanism of catalysis as is the very fast so-called "kissing ribozyme" reaction described by Khvorova et al.[57]

Experimental Section

Preparation of the Hammerhead Ribozyme and Substrate. The ribozyme (R32) and its substrate (S11) were synthesized chemically on a DNA/RNA synthesizer (model 394; PE Applied Biosystems, Foster City, CA) using phosphoramidic chemistry with 2′-*tert*-butyldimethylsilyl (TBDMS) protection, as described elsewhere.[47] The chemically synthesized oligonucleotides R32 and S11 were deprotected by incubation in a mixture of 28% ammonia and ethanol (3:1, v/v) at 55 °C for 8 h. Each mixture was evaporated to dryness, and the residue was allowed to dissolve in 1 mL of 1 M tetrabutylammonium fluoride (TBAF; Sigma-Aldrich Japan K. K., Tokyo, Japan) at room temperature for 12 h. After the addition of 1 mL of water, the mixture was desalted on a gel-filtration column (Bio-Gel P-4; Bio-Rad Laboratories, Hercules, CA). Fully deprotected oligonucleotides were purified by gel electrophoresis on a 20% polyacrylamide gel that contained 7 M urea, the respective bands were excised from the gel, and oligonucleotides were extracted in water. The oligonucleotides were recovered by ethanol precipitation, and then solutions were desalted on a gel-filtration column (TSK-GEL G3000PW; TOSOH, Tokyo, Japan) with ultrapure water. The RNA oligomers were quantitated in terms of absorbance at 260 nm.

We radiolabeled the substrate S11 using [γ-^{32}P]-ATP and T4 polynucleotide kinase (TaKaRa Bio Inc., Shiga, Japan) and purified the radiolabeled S11 on a 20% polyacrylamide gel that contained 7 M urea. After purification by the standard procedure as described above, the preparation of S11 was desalted on a gel-filtration column (NAP-10 column; Amersham Biosciences K. K., Tokyo, Japan).

Quantification of the Ribozyme Reaction. All ribozyme reactions were performed under ribozyme-saturated single-turnover conditions to ensure that conversion of the ribozyme–substrate complex to the ribozyme–product complex could be monitored kinetically without complications due to complex formation and slow release of product in particular at a high concentration of metal ions. The solution for the ribozyme reaction contained a trace amount of 5′-^{32}P-labeled S11 in 25 mM Bis-Tris buffer at pH 6.0 or pH 7.5 and 25 °C. The pH values of all 1.25× stock Bis-Tris buffers that contained appropriate metal ions (metal-ion buffers) were adjusted appropriately with HCl, and we confirmed that each buffer had the appropriate pH under the chosen reaction conditions. The error in the reading of pH meter under very high concentrations of metal ions is expected to be negligible.[58] Each reaction was initiated by addition of the substrate to a mixture of metal-ion buffer and ribozyme, and aliquots were removed from the reaction mixture at appropriate intervals. Each aliquot was mixed with more than three volumes of a stop solution that contained 100 mM MES (pH 6), 100 mM EDTA, 7 M urea, xylene cyanol (0.1%), and bromophenol blue (0.1%), and then it was stored at −80 °C prior to analysis. Since EDTA is known not to chelate Mg^{2+} ions efficiently at lower pH values and does not effectively chelate monovalent cations, we confirmed that reactions did not continue in the stop solution and that effective quenching was achieved as a result of the high concentration of urea in this solution. Uncleaved substrate and 5′-cleaved products were separated on a 20% polyacrylamide gel that contained 7 M urea. The extent of each cleavage reaction was quantitated with an image analyzer (Storm 830; Molecular Dynamics, Sunnyvale, CA). For each reaction, an observed rate constant was determined by nonlinear least-squares fitting of the time course of the reaction, using the following pseudo-first-order equation:

$$P_t = P_e - (P_e - P_0)\exp(-k_{obs}t)$$

where P_t is the amount of a product at reaction time t (min), P_e is the amount of a product at the endpoint, P_0 is the amount of a product at the start of the reaction, and k_{obs} is the observed rate constant (min^{-1}).

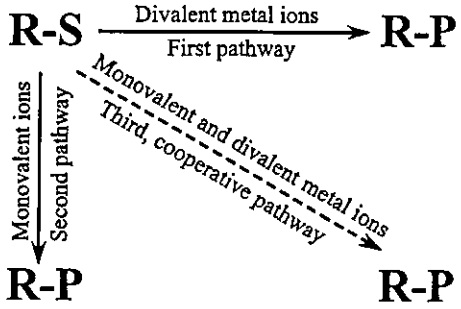

Figure 2. Possible pathways in the hammerhead ribozyme reaction. R–S and R–P stand for the ribozyme–substrate complex and the ribozyme–product complex, respectively. The first pathway requires only divalent metal ions, such as Mg^{2+} ions; the second pathway requires monovalent ions, such as Li^+ ions; and the third pathway involves both divalent and monovalent cations.

The Basic Strategy for the Establishment of the Pathways of Reactions Catalyzed by the Hammerhead Ribozyme. The basic strategy for establishment of the pathways of the reaction is shown in Figure 2. We suggested previously that a third pathway might be operative in the ribozyme reaction in addition to the two that have already been well characterized.[50] The first and second pathways involve only Mg^{2+} ions and only Li^+ ions, respectively. The third pathway involves the cooperative effects of two kinds of metal ion. We first investigated the dependence of the reaction on either Mg^{2+} or Li^+ ions independently and fitted the results to each scheme that has been postulated on the basis of our earlier data to choose values for basic parameters by nonlinear least-squares method. Finally, we established the third pathway on the basis of the reaction that occurred in the presence of the two metal ions, proceeding step by step and satisfying the parameters established in our analyses of the first and second pathways.

Results and Discussion

Li^+ Ions Have an Inhibitory Effect but Are Also a Better Accelerator Than Other Monovalent Ions of the Ribozyme Reaction in the Presence of Mg^{2+} Ions. We examined the activity of the hammerhead ribozyme as a function of the concentration of various monovalent metal ions, namely, Li^+, Na^+, K^+, Cs^+, and NH_4^+ in the presence of 10 mM Mg^{2+} ions. The reactions were performed at pH 6 and 25 °C, at concentrations on monovalent cations from 0 to 3 M. As shown in Figure 3, all monovalent ions, the Group I metal ions and NH_4^+ ions, had an inhibitory effect at a few hundred mM in the presence of 10 mM Mg^{2+} ions. This inhibitory effect can be explained by the simple hypothesis that monovalent ions prevent necessary binding of Mg^{2+} ions to the ribozyme–substrate complex, as validated by DeRose and colleagues by EPR.[53]

In the case of Li^+, Na^+, and NH_4^+ ions, the ribozyme activity was elevated at higher concentrations of each monovalent ion individually. This observation is consistent with our previous observations of reactions in the presence of either Mn^{2+} plus Na^+ ions or Mg^{2+} plus Na^+ ions.[50] The inhibitory effect of Na^+ ions has also been observed in kinetic studies by other

(57) Khvorova, A.; Lescoute, A.; Westhof, E.; Jayasena, S. D. *Nat. Struct. Biol.* **2003**, *10*, 708–712.
(58) Millazo, G. *Elektrochemie*; Springer-Verlag: Berlin, 1952; p 98.

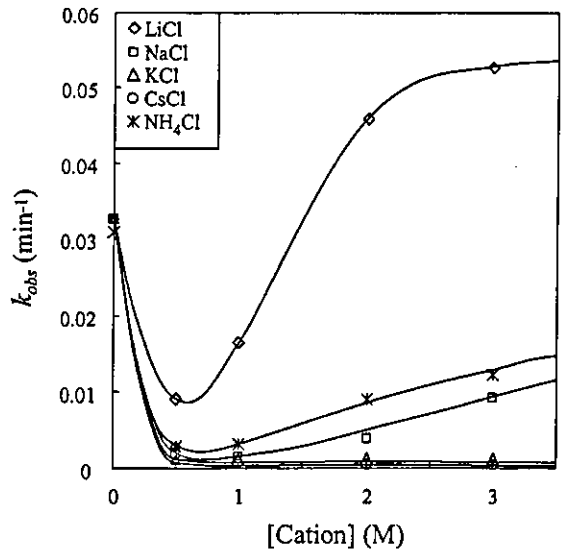

Figure 3. Dependence on various monovalent ions of the activity of the hammerhead ribozyme (R32) in the presence of Mg^{2+} ions. Values of k_{obs} are plotted as a function of concentration of Li^+, Na^+, K^+, Cs^+, and NH_4^+ ions, respectively. All reactions were performed in the presence of 10 mM Mg^{2+} ions under ribozyme-saturated single-turnover conditions at pH 6 and 25 °C. All monovalent ions had an inhibitory effect at 500 mM, and Li^+ ions accelerated the reaction at higher concentrations.

researchers at 100 mM Na^+ ions in the presence of Mg^{2+} ions.[59] In addition to their inhibitory effect, Li^+ ions at higher concentrations were the best accelerator of the ribozyme reaction in the presence of Mg^{2+} ions.

In the case of K^+ and Cs^+ ions, respectively, there was no acceleration of the reaction and both ions had the same effect (Figure 3). The rank order, in terms of the acceleration of ribozyme activity of the various monovalent ions in the presence of Mg^{2+} ions, was rather similar to that of these monovalent ions in the absence of divalent metal ions (data not shown). As noted by Curtis and Bartel,[37] such dependence is correlated with the radius of each anhydrous ion and appears to be manifested even on a background of Mg^{2+} ions (Figure 3).

It is particularly noteworthy that the observed accelerated activities were higher than the calculated sums of the activities in the presence of Li^+ ions and in the presence of Mg^{2+} ions, suggesting that the divalent and monovalent ions act cooperatively in the reaction catalyzed by the hammerhead ribozyme (Figure 3).[50] We chose the combination of Mg^{2+} and Li^+ ions for further stoichiometric analysis since it yielded the most pronounced profile in terms of inhibition and acceleration and the highest activities of all the combinations that we tested (Figure 3).

The Mg^{2+}-Mediated Ribozyme Reaction and Elucidation of the First Pathway. We examined the dependence on Mg^{2+} ions of the activity of the hammerhead ribozyme up to a concentration of Mg^{2+} ions close to 1 M at pH 6 and 25 °C under single-turnover conditions (ribozyme-saturating with respect to the substrate) to ensure that the kinetics of the cleavage reaction could be monitored without complications due to formation of the ribozyme–substrate complex and the slow release of products. As reported previously, the reaction in the presence of Mg^{2+} ions is accelerated by increases in pH with a slope of unity.[36,44,60–62] Thus, we adjusted the pH of the reactions in this study to 6.0 to slow the reaction. Under these conditions, we were able to measure the rate constant of the rapid reaction precisely.

As shown in Figure 4A, we found an approximately first-order dependence on the concentration of Mg^{2+} ions, and the rate constant did not reach a plateau value under our conditions, even at more than 800 mM Mg^{2+} ions. The continuous increase in the rate constant with the addition of more and more Mg^{2+} ions indicates the involvement of a Mg^{2+} ion that has very low affinity for the hammerhead ribozyme–substrate complex. At 800 mM Mg^{2+} ions, the rate constant approached 1 min^{-1} at pH 6 and 25 °C, which is the limit of detection of a rapid cleavage reaction under standard laboratory conditions. The dependence of the activities of the hammerhead ribozymes on Mg^{2+} ions has been studied by many researchers, generally of concentrations of Mg^{2+} ions below 200 mM.[59–61,63,64] In most cases, the rate constant reached or approached a plateau value.[59,60,63] In this respect, our ribozyme exhibits unusual dependence on Mg^{2+} ions.

Earlier analyses of the structure of hammerhead ribozymes and of the conformational changes caused by interactions with Mg^{2+} ions suggested that major conformational changes occur in two stages, with the formation of domain II and then domain I, as indicated in Figure 1C.[52,54–56] The formation of domain II occurs first and results in the coaxial stacking of helices II and III. This conformational change is induced by the binding of a higher-affinity Mg^{2+} ion(s) to the ribozyme–substrate complex. A divalent metal ion bound to the A9/$G_{10.1}$ site is a strong candidate for the ion that is involved in this first transition.[47d,65,66]

The second conformational change is the formation of the catalytic domain of the ribozyme, with movement of stem I toward stem II, and this change is induced by the binding of a lower-affinity Mg^{2+} ion(s). The K_d (equilibrium dissociation constant) of each transition has been investigated by various methods and appears to be several hundred micromolar and several millimolar for the first and the second transition, respectively.[52–56] Therefore, we chose 100 μM and 1 mM as K_{d1} and K_{d2}, the fixed dissociation constants of the first and the second Mg^{2+} ion(s), respectively, for the fitting in the first pathway (Figures 1C, 2, and 4B). The ribozyme reaction in the presence of high concentrations of Mg^{2+} ions did not reach saturation. Therefore, we included additional Mg^{2+} ions (indicated as x Mg^{2+}) in the pathway, as shown in Figure 4B, and we fitted the reaction profiles to the following equation:

$$k_{obs} = \frac{\dfrac{[Mg^{2+}]^{(2+x)}}{K_{d1}K_{d2}K_{d6}}}{1 + \dfrac{[Mg^{2+}]}{K_{d1}} + \dfrac{[Mg^{2+}]^2}{K_{d1}K_{d2}} + \dfrac{[Mg^{2+}]^{(2+x)}}{K_{d1}K_{d2}K_{d6}}} k_1$$

where K_{d6} is the dissociation constant of the additional Mg^{2+}

(59) Rueda, D.; Wick, K.; McDowell, S. E.; Walter, N. G. *Biochemistry* **2003**, *42*, 9924–9936.
(60) Dahm, S. C.; Derrick, W. B.; Uhlenbeck, O. C. *Biochemistry* **1993**, *32*, 13040–13045.
(61) Hendry, P.; McCall, M. J. *Nucleic Acids Res.* **1995**, *23*, 3928–3936.
(62) Peracchi, A. *Nucleic Acids Res.* **1999**, *27*, 2875–2882.
(63) (a) Kuimelis, R. G.; McLaughlin, L. W. *Biochemistry* **1996**, *35*, 5308–5317. (b) Hunsicker, L. M.; DeRose, V. J. *J. Inorg. Biochem.* **2000**, *80*, 271–281.
(64) Hampel, K. J.; Burke, J. M. *Biochemistry* **2003**, *42*, 4421–4429.
(65) DeRose V. J. *Curr. Opin. Struct. Biol.* **2003**, *13*, 317–324.

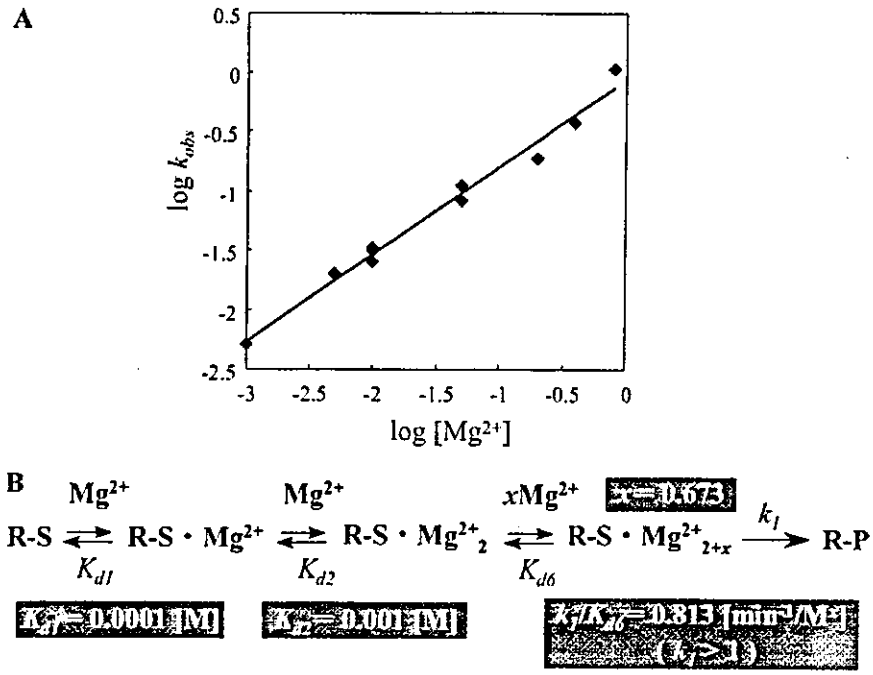

Figure 4. (A) Dependence on Mg^{2+} ions of the activity of the hammerhead ribozyme (R32). All reactions were performed at pH 6 and 25 °C under ribozyme-saturated single-turnover condition. The concentration of Mg^{2+} ions ranged from 1 mM to 800 mM. The theoretical curve (– – –) as drawn after parameters had been fitted to the equation given in the text. (B) The first pathway, involving Mg^{2+} ions, of the ribozyme reaction. R–S stands for the ribozyme–substrate complex. All parameters are explained in the text.

ion(s), k_1 is the rate constant for cleavage at a saturating concentration of Mg^{2+} ions, and x is the additional number of Mg^{2+} ions.

Since the reaction did not reach saturation even at 800 mM Mg^{2+} ions, we could not define k_1 and K_{d6}, but we were able to determine the values of k_1/K_{d6} and x after fitting the results to the equation. The calculated values of k_1/K_{d6} and x were 0.813 [min^{-1}/M^x] and 0.673, respectively. However, k_1 must be greater than 1 because k_{obs} is close to 1 min^{-1} at 800 mM Mg^{2+} (k_{obs} should be nearly equal to k_1 at saturating concentration of Mg^{2+} ions). The theoretical curve, obtained after putting these results in the equation, is shown in Figure 4A.

At several hundred millimolar Mg^{2+} ions, the formation of both domains II and I would be complete because of the low values of K_{d1} and K_{d2}. If we take the global changes induced by the two types of Mg^{2+} ion into consideration, it seems reasonable to conclude that the Mg^{2+} ion with very low affinity that we detected might be involved in some step other than the formation of domains II and I. The step might be a further conformational change or the binding of a catalytic species to the ribozyme–substrate complex. Rueda et al. reported that a third and previously undetected metal ion at a rather high concentration might play a role in the induction of a minor conformational adjustment that leads to formation of the active state, after the formation of domains II and I.[59]

Although we are unable to calculate a Hill coefficient for Mg^{2+} ions and cannot estimate the number of Mg^{2+}-binding sites from our current data, our results and those of others strongly support the possible existence of a very-low-affinity metal-binding site(s). Misra and Draper propose a model for the stabilization of RNA by Mg^{2+} ions that involves two distinct binding modes, "diffuse binding" and "site binding".[67] Diffusely bound Mg^{2+} ions are described as fully solvated Mg^{2+} ions that interact with RNA through long-range electrostatic interactions exclusively. Site-bound Mg^{2+} ions are described as partially desolvated ions that are attracted to electronegative pockets. In general, the affinity of diffusely bound Mg^{2+} ions seems to be lower than that of site-bound Mg^{2+} ions. Thus, it is possible that the very-low-affinity Mg^{2+} ions that we detected might be involved in diffuse binding. Diffuse binding of metal ions appears, sometimes, to play a dominant role in the stabilization of the tertiary structures of small RNAs,[67] but it might also participate in the ribozyme reaction at some specific site(s) in the ribozyme–substrate complex.

The activity of the hammerhead ribozyme in 800 mM Mg^{2+} ions is unusual because the observed rate constant is estimated to be about 100 min^{-1} at pH 8 and 25 °C from the dependence on pH, which has a slope of unity as noted above. The rate constant at concentrations of Mg^{2+} ions above 800 mM should be even higher because it is clear that 800 mM Mg^{2+} is not a saturating concentration for the cleavage reaction. The rate constant approaches the estimated observed rate constant for the so-called "kissing ribozyme" at optimum conditions with respect to a concentration of Mg^{2+} ions and pH.[57] The Mg^{2+} ion has very low affinity for the ribozyme–substrate complex, and the number of truly active ribozyme species, at concentrations of Mg^{2+} ions of several millimolar, is less than 1% of the number of ribozyme–substrate complexes (compare 1 min^{-1} in 10 mM $MgCl_2$ at pH 8 and 25 °C[68] with 100 min^{-1} in 800 mM $MgCl_2$ at the same pH and the same temperature).

The Li^+-Mediated Ribozyme Reaction and Elucidation of the Second Pathway. We examined the activity of the hammerhead ribozyme as a function of the concentration of Li^+

(66) Tanaka, Y.; Kasai, Y.; Mochizuki, S.; Wakisaka, A.; Morita, E. H.; Kojima, C.; Toyozawa, A.; Kondo, Y.; Taki, M.; Takagi, Y.; Inoue, A.; Yamasaki, K.; Taira, K. *J. Am. Chem. Soc.* **2004**, *126*, 744–752.

(67) Misra, V. K.; Draper, D. E. *J. Mol. Biol.* **2002**, *317*, 507–521.

(68) Stage-Zimmermann, T. K.; Uhlenbeck, O. C. *RNA* **1998**, *4*, 875–889.

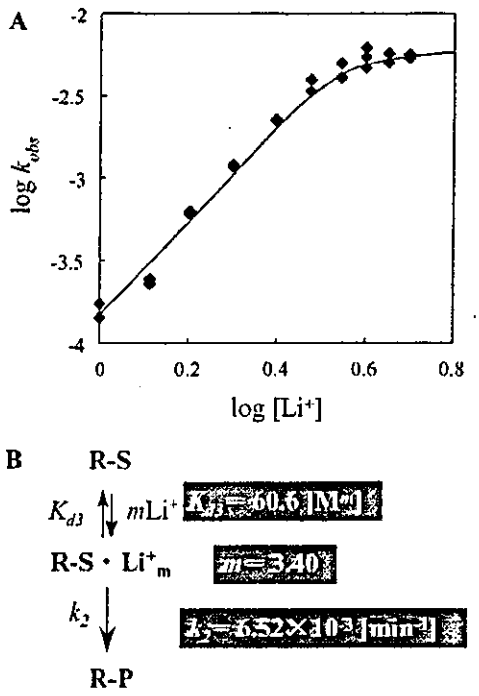

Figure 5. (A) Dependence on Li^+ ions of the activity of the hammerhead ribozyme (R32) at pH 6. All reactions were performed at pH 7.5 and 25 °C under the ribozyme-saturated single-turn over conditions and the concentration of Li^+ ions ranged from 1 to 5 M. Data at pH 6 were extrapolated from the experimental data obtained at pH 7.5 as described in the text. The theoretical curve (——) was drawn after parameters had been fitted to the equation given in the text. (B) The second pathway, involving Li^+ ions, of the hammerhead ribozyme reaction. R—S stands for the ribozyme—substrate complex. All parameters are explained in the text.

ions, in the absence of divalent metal ions, under ribozyme-saturating single-turnover conditions at pH 7.5 and 25 °C. The experimental data obtained at pH 7.5 were extrapolated to give results at pH 6 on the basis of the fact that the dependence of activity on pH has a slope of unity.[37,50b] The results are shown by diamonds in Figure 5A.

It is clear that the slope of the linear part of the curve in Figure 5A is steeper than that in Figure 4A (in the presence of Mg^{2+} ions) and the activity reaches a plateau at high concentrations of Li^+ ions. Using the simple pathway shown in Figure 5B, we fitted the data to the following equation:

$$k_{obs} = \frac{\frac{[Li^+]^m}{K_{d3}}}{1 + \frac{[Li^+]^m}{K_{d3}}} k_2$$

where m is the number of Li^+ ions, K_{d3} is the dissociation constant of Li^+ ions, and k_2 is the rate constant for cleavage under Li^+-saturating conditions. The data fit well when m = 3.40, K_{d3} = 60.6 M^m, and $k_2 = 6.52 \times 10^{-3}$ min^{-1} at pH 6. The theoretical curve obtained after fitting these values is shown in Figure 5A.

O'Rear et al. reported that the hammerhead reaction has second-order dependence on Li^+ ions, without a plateau.[38] By contrast, our ribozyme exhibited more than third-order dependence, and a plateau was observed (Figure 5A). Although there are some differences between our results and those of O'Rear et al., in both cases the order of dependence on Li^+ is greater than that on Mg^{2+} ions, suggesting that Li^+ ions bind cooperatively to the ribozyme—substrate complex, while Mg^{2+} ions bind sequentially.

From the value of k_2 at pH 7.5 and 25 °C, we recalculated the value at pH 6 and 25 °C (again, the ribozyme reaction is dependent, with a slope of a unity, on pH at high concentrations of Li^+ ions).[50b] We estimated k_2 to be 6.52×10^{-3} min^{-1} at pH 6 and 25 °C and used this value for stoichiometric analysis of the third pathway (see below).

The Hammerhead Ribozyme Reaction in the Presence of Mg^{2+} and Li^+ Ions and Characterization of the Third, Cooperative Pathway. To characterize the third pathway, we examined the rate constant of the ribozyme reaction as a function of the concentration of Mg^{2+} ions on a background of 2 M Li^+ ions and as a function of the concentration of Li^+ ions on a background of 10 mM Mg^{2+} ions. All reactions were performed under ribozyme-saturating single-turnover conditions at pH 6 and 25 °C. The results are shown in Figure 6A,B. Parts A and B of the figure show apparent saturation at a high concentration of either Mg^{2+} or Li^+ ions. We tested many possible third pathways for a good fit to these data, using the parameters of the first and second pathways that we had already fixed. We were able to identify a third, cooperative pathway that satisfied all the experimental data. The entire scheme, including the first, second, and third pathways, is shown in Figure 6C, and the corresponding equation is as follows:

$$k_{obs} = f_1 k_1 + f_2 k_2 + f_3 k_3$$

where

$$f_1 = \frac{1}{g} \cdot \frac{[Mg^{2+}]^{(2+x)}}{K_{d1} K_{d2} K_{d6}}$$

$$f_2 = \frac{1}{g} \cdot \frac{[Li^+]^m}{K_{d3}}$$

$$f_3 = \frac{1}{g} \cdot \frac{[Mg^{2+}]^{(1+y)}[Li^+]^{(n+n')}}{K_{d1} K_{d4} K_{d5} K_{d7}}$$

$$g = 1 + \frac{[Mg^{2+}]}{K_{d1}} + \frac{[Mg^{2+}]^2}{K_{d1}K_{d2}} + \frac{[Li^+]^m}{K_{d3}} + \frac{[Mg^{2+}][Li^+]^n}{K_{d1}K_{d4}} + \frac{[Mg^{2+}][Li^+]^{(n+n')}}{K_{d1}K_{d4}K_{d5}} + \frac{[Mg^{2+}]^{(2+x)}}{K_{d1}K_{d2}K_{d6}} + \frac{[Mg^{2+}]^{(1+y)}[Li^+]^{(n+n')}}{K_{d1}K_{d4}K_{d5}K_{d7}}$$

and where n is the number of Li^+ ions as indicated in Figure 6C, K_{d4} is the dissociation constant of these n Li^+ ions, n' is the number of further additional Li^+ ions as indicated in Figure 6C, K_{d5} is the dissociation constant of these n' Li^+ ions, y is the number of Mg^{2+} ions indicated in Figure 6C, K_{d7} is the dissociation constant of these y Mg^{2+} ions, and k_3 is the rate constant for cleavage in the third pathway.

The third pathway involves interactions of Mg^{2+} ions and Li^+ ions with the ribozyme—substrate complex. In the third pathway, n Li^+ ions compete with a Mg^{2+} ion (in the first pathway) to form a R—S·Mg^{2+}·Li^+_n complex. This competition is the main cause of the observed inhibitory effect (Figure 3; see also below for details). Upon addition of more Li^+ ions, the relative activity of the first Mg^{2+}-only pathway becomes

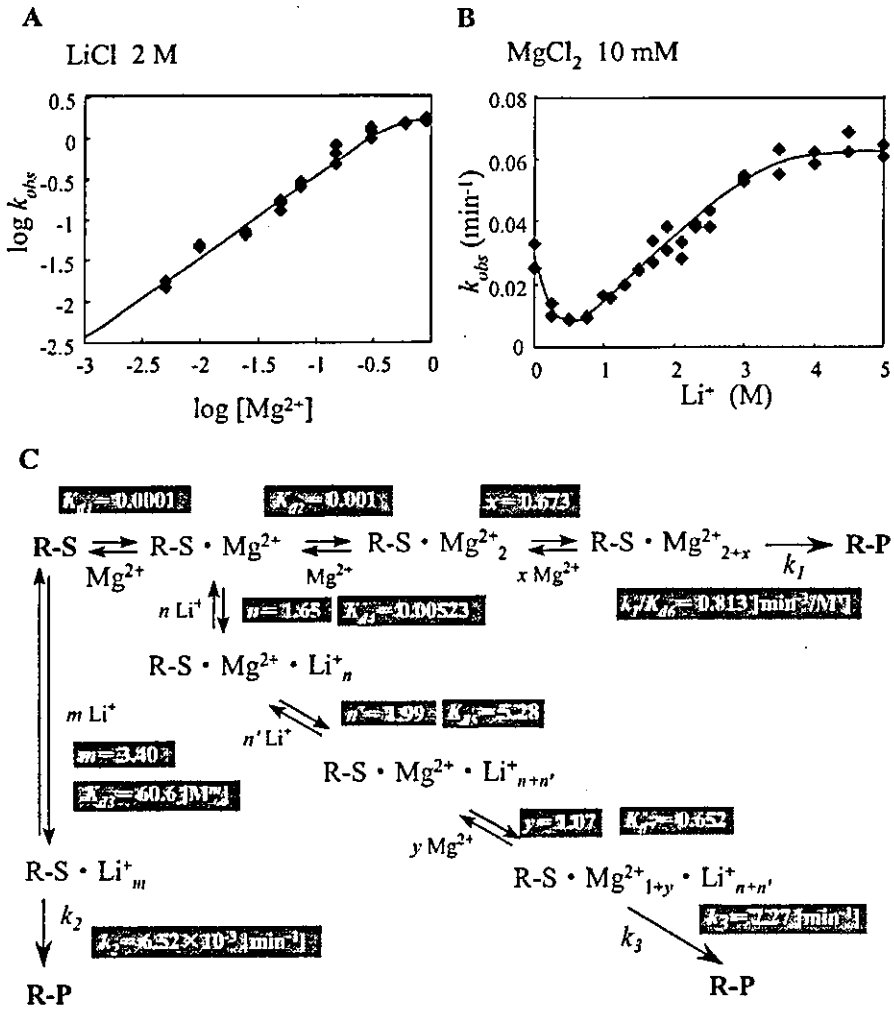

Figure 6. (A) Dependence on Mg^{2+} ions of the activity of the hammerhead ribozyme (R32) in the presence of 2 M Li^+ ions. All reactions were performed at pH 6 and 25 °C under the ribozyme-saturated single-turnover conditions and the concentration of Mg^{2+} ions ranged from 5 mM to 800 mM. The theoretical curve (– – –) was drawn after parameters had been fitted to the equation given in the text. (B) Dependence on Li^+ ions of the activity of the hammerhead ribozyme (R32) on a background of 10 mM Mg^{2+} ions. All reactions were performed at pH 6 and 25 °C under the ribozyme-saturated single-turnover conditions at concentration of Li^+ ions that ranged from 0 to 5 M. The theoretical curve (– – –) was drawn after parameters had been fitted to the equation given in the text. (C) The third pathway, involving both Li^+ and Mg^{2+} ions, for the ribozyme reaction at pH 6 and 25 °C. R–S and R–P stand for complexes of the ribozyme–substrate and the ribozyme–product, respectively. All parameters are explained in the text.

smaller. We might imagine that the second Li^+-only pathway would become the major pathway upon addition of more Li^+ ions. However, the activity, indicated by k_2, of the second pathway is much lower than the Mg^{2+}-based rate, and the affinity of Li^+ ions for the ribozyme–substrate complex in the second pathway is very low.

Thus, the third cooperative pathway, instead of the second pathway, becomes the major pathway upon addition of more Li^+ ions. The R–S·Mg^{2+}·Li^+_n complex is converted to a R–S·Mg^{2+}·$Li^+_{(n+n')}$ (Figure 6C) upon binding of n' Li^+ ions. We then added y Mg^{2+} ions to the R–S·Mg^{2+}·$Li^+_{(n+n')}$ complex because we failed to obtain a good fit without the addition of such Mg^{2+} ions. Thus, in the third pathway, two different metal ions, namely $(1+y)$ Mg^{2+} ions and $(n+n')$ Li^+ ions, are involved in formation of the final complex. Using this model, we fit all the data to the equation and obtained by nonlinear least-squares method the following values: $n = 1.65$, $K_{d4} = 0.00523$, $n' = 1.99$, $K_{d5} = 5.28$, $y = 1.07$, $K_{d7} = 0.652$, and $k_3 = 7.27$ at pH 6 and 25 °C (Figure 6C).

The theoretical curves, obtained after inserting these parameters in the equation, are shown in Figure 6A,B. If we assume that k_1 is 1 min^{-1} (this value is an underestimate because the reaction did not reach saturation even at 800 mM Mg^{2+} ions; see above), the relative extent of each pathway on a background of Mg^{2+} ions is as follows: 100% via the first pathway at 0 M Li^+ ions; 92% via the first pathway and 8% via the third pathway at 500 mM Li^+ ions; 48% via the first pathway and 52% via the third pathway at 1 M Li^+ ions; and 100% via the third pathway at 5 M Li^+ ions (Figure 7).

These parameters imply that (i) the pathway involving Li^+ ions alone (the second pathway) is negligible when both Li^+ and Mg^{2+} ions are available (Figure 7A,B), (ii) an increase in the concentration of Li^+ ions on a background of Mg^{2+} ions induces cooperation between Li^+ and Mg^{2+} ions (the third pathway; Figure 7A), and (iii) an increase in the concentration of Mg^{2+} ions on a background of Li^+ ions induces cooperation between Li^+ and Mg^{2+} ions (the third pathway), although higher concentrations of Mg^{2+} ions induce the first pathway and dramatically reduce the activity of the third pathway (Figure 7B). Simulations made on the assumption that k_1 is 5 or 10 min^{-1} (rather than 1 min^{-1}) did not affect these conclusions. It should also be emphasized that, in the measurements of reaction

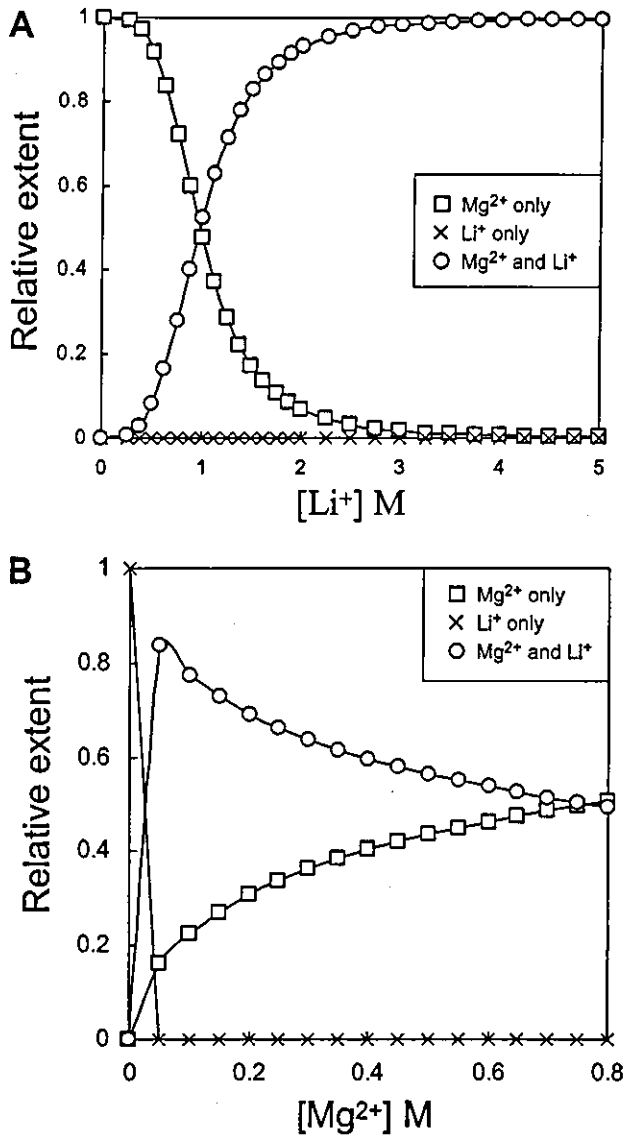

Figure 7. Simulations showing the relative extent of involvement of each of the three pathways in the proposed scheme for hammerhead ribozyme reactions. The first pathway involved only Mg^{2+} ions (□), the second pathway involved only Li^+ ions (×), and the third pathway involved both Li^+ and Mg^{2+} ions (○). In this scheme, k_1 was taken as 1 min^{-1}. The relative values were obtained from calculations of f_1 (Mg^{2+} alone), f_2 (Li^+ alone), and f_3 (Mg^{2+} and Li^+; see the equations in the text) after fitting of the various parameters. (A) Simulation, in the presence of 10 mM Mg^{2+} ions, of the relative extent of involvement of each pathway as a function of the concentration of Li^+ ions. (B) Similar simulations performed as a function of the concentration of Mg^{2+} ions in the presence of 2 M Li^+ ions.

rates summarized in Figure 6C, we were unable to adjust the ionic strength at each concentration of metal ions because different cations we tested had differently affected the ribozyme reaction, as shown in Figure 3. Although we cannot exclude the possibility that the obtained parameters might have been influenced by the ionic strength, the major finding that the ribozyme reaction can proceed by a new cooperative pathway involving both monovalent and divalent metal ions remains valid.

Comparison of Our Data with Previous Data. In a previous report, we suggested the possible existence of various catalytic channels for the hammerhead ribozyme, depending on the reaction conditions. For example, a Mg^{2+} ion functions as a catalyst in the transition state in Mg^{2+}-containing solutions while an NH_4^+ ion functions as a catalyst in NH_4^+-containing solutions.[51] Our data support an anhydrate direct interaction between these ions and the 5′-leaving oxygen atom at the cleavage site.[51]

However, since $Co(NH_3)_6^{3+}$ ions enhance the ribozyme's activity, we cannot exclude the possibility that, for example, a hydrated cation also functions as a catalyst in the transition state.[66] A multiple-channel model has also been proposed for reactions catalyzed by the HDV genomic ribozyme in which a base catalyst changes according to the environment in which the HDV ribozyme reaction occurs.[35] We propose similarly that several pathways are possible in the reaction catalyzed by hammerhead ribozymes. One of the pathways, the cooperative pathway, involves several different cations simultaneously. In the case of the reaction catalyzed by the RNA subunit of RNase P, similar cooperativity by Mg^{2+} and Ca^{2+} ions has been reported.[69]

Our data also suggest the existence of a very-low-affinity Mg^{2+} ion (corresponding to K_{d6} in Figures 4B and 6C), which was not included in the "two-phase folding model" proposed by Lilley and co-workers.[52,54-56] In a previous report, we postulated that this very-low-affinity Mg^{2+} ion might play a catalytic or a structural role.[50] Rueda et al. reported recently that a third Mg^{2+} ion might play a role, at a rather high concentration, in a minor conformational adjustment that results in formation of the active state after the formation of domains II and I (Figure 1C).[59] The Mg^{2+} ion that we detected in the present study might be the same as the Mg^{2+} ion that they discussed.

Our ribozyme did not yield a plateau even at 800 mM Mg^{2+} ions (Figure 4A), while HHα (another hammerhead ribozyme that has been used in studies of reaction mechanisms by other researchers) yields a plateau at 100 mM Mg^{2+} ions.[59] Breaker and co-workers proposed recently that a speed limit might exist for RNA-cleaving ribozymes that adopt $\alpha\gamma$ catalytic strategies, when the α, β, γ, and δ steps in catalysis are equivalent, respectively, to in-line nucleophilic attack, neutralization of negative charge on a nonbridging oxygen atom, deprotonation of the 2′-hydroxyl group, and neutralization of negative charge on the 5′-oxygen atom.[70,71] The reaction catalyzed by our hammerhead ribozyme cannot be categorized in terms of these steps because the k_{max} of the reaction under optimal conditions can be extrapolated to exceed the speed limit of $\alpha\gamma$ catalysis at neutral pH and 25 °C (see above). This observation suggests the existence of some other catalytic strategy, for example, a δ-metalation strategy or a β-metalation strategy. We noted earlier that no direct interaction occurs between a nonbridging oxygen atom and Mg^{2+} ions at the cleavage site during cleavage by the hammerhead ribozyme,[47] while the direct coordination of a Mg^{2+} ion to the 5′-leaving oxygen atom in the transition state was realized.[44,49,51] Thus, it appears that the hammerhead ribozyme exploits an $\alpha\gamma\delta_{metalation}$ strategy, rather than an $\alpha\beta_{metalation}\gamma$ strategy in Mg^{2+}-containing solutions. While this scenario might be valid in the Mg^{2+}-mediated ribozyme reaction, we cannot ignore the possibility that the same hammerhead

(69) Brännvall, M.; Kirsebom, L. A. *Proc. Natl. Acad. Sci. U.S.A.* **2001**, *98*, 12943−12947.
(70) Emilsson, G. M.; Nakamura, S.; Roth, A.; Breaker, R. R. *RNA* **2003**, *9*, 907−918.
(71) Breaker, R. R.; Emilsson, G. M.; Lazarev, D.; Nakamura, S.; Puskarz, I. J.; Roth, A.; Sudarsan, N. *RNA* **2003**, *9*, 949−957.

ribozyme might adopt a different strategy in a different environment.[51]

Rueda et al. reported that Na^+ ions had an inhibitory effect on the HHα ribozyme at 100 mM Na^+ ions on a background of Mg^{2+} ions.[59] Hendry and McCall also reported the inhibitory effect on their hammerhead ribozyme of Na^+ ions on a background of Mg^{2+} ions.[61] Such effects are consistent with our previous and current observations, namely, that inhibitory effects are greater at 500 mM Na^+ ions in the presence of a low concentration of Mg^{2+} or Mn^{2+} ions. However, the activity of our ribozyme can be restored by the addition of high concentrations of K^+ ions, Na^+ ions, or Li^+ ions (Figures 3 and 6B).[50] The activity of our ribozyme depended on the concentration of Mg^{2+} ions even at around 1 M Mg^{2+} ions. The observed rate constant of ~1 min^{-1} at pH 6 and 25 °C in 800 mM Mg^{2+} ions under single-turnover conditions allowed us to estimate that the ribozyme activity would be 100 min^{-1} at pH 8. Since we observed no sign of saturation by Mg^{2+} ions (Figure 4A), concentrations of Mg^{2+} ions above 800 mM should lead to a rate constant greater than 100 min^{-1} at pH 8. This rate constant is similar to that of the so-called "kissing ribozyme with the optimum activity" under optimum conditions with respect to a concentration of Mg^{2+} ions and pH.[57]

Conclusions

We have established a novel third pathway, namely, a cooperative pathway that involves monovalent and divalent metal ions, for the hammerhead ribozyme reaction. Moreover, complete kinetic parameters were obtained that explain the ribozyme activities under different conditions. The ribozyme reaction is more complex than might have been expected, perhaps because of the flexibility of RNA, which would have enhanced the potential of RNA during evolution of and in the RNA world. Our ribozyme, used as a model, might mimic the chemical cleavage of the so-called "kissing ribozyme with the optimum activity" because there was no upper limit to the rate constant of cleavage even at high concentrations of Mg^{2+} ions. Further studies with our ribozyme might help to elucidate the catalytic mechanism of the "kissing ribozyme". Our analysis further indicates that the high concentrations of monovalent ions are inhibitory for the ribozyme in cells that is the disadvantage to the ribozyme compared to other catalysts such as siRNA whose activity can be enhanced by intracellular factors.

JA031991U